

ESCA: electron spectroscopy for chemical analysis

Summer School „Methods in Surface Science“
Clausthal-Ljubljana

October 20, 2025

Scope of this lecture

Typical questions addressed by materials scientists:

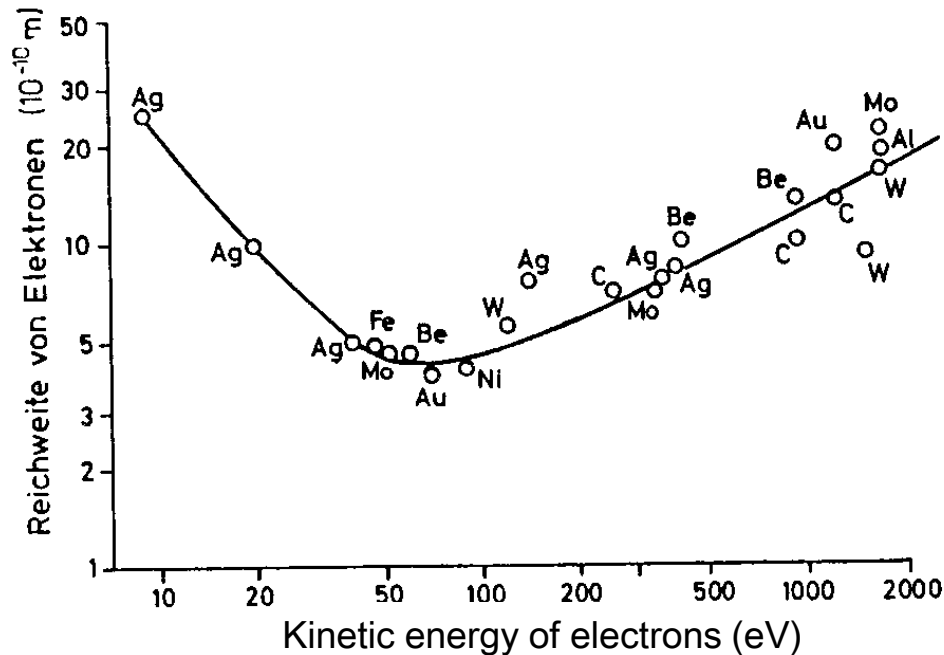
- What is the chemical composition of a material's surface?
- Is the composition at the surface different from that in the bulk?
- Is the surface „clean“ or covered with a contamination layer or a surface oxide
- How does the chemical composition vary across the surface?
- Are there precipitations of different materials at the surface?
- Is chemical bonding at the surface different from that in the bulk?

Surface-sensitive probes with an information depth of only few atomic layers are needed to address these questions

- Common photonic probes (IR and Raman spectroscopy, UV-vis-spectroscopy, X-ray fluorescence) lack this sensitivity in general



Low energy electrons are very surface sensitive! 😊



Range λ of electrons:

$$I(x) = I_0 e^{-(x/\lambda)}$$

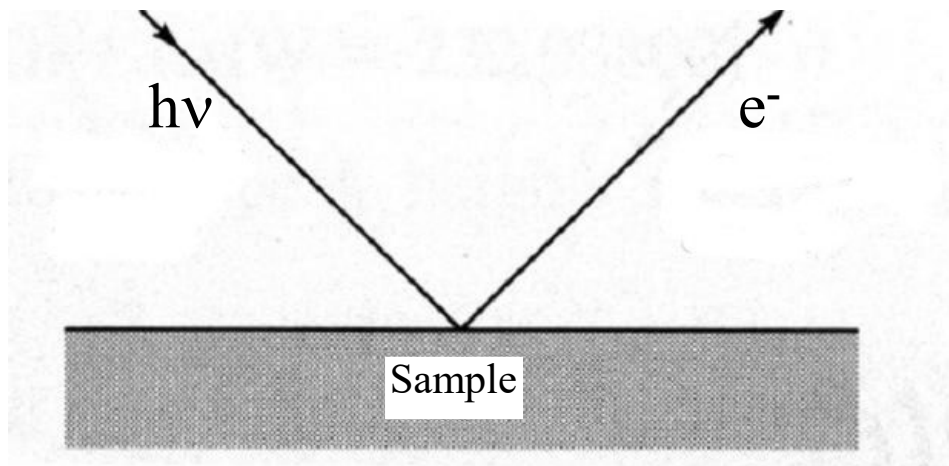
See, e. g.,
M.P. Seah, W.A. Dench,
Surf. Interf. Analysis I (1979)

- Between 10 and 2000 eV kinetic energy the range / escape depth λ of electrons is less than 2 nm
- Between 20 and 1000 eV kinetic energy less than 1 nm
- Between 40 and 100 eV only 0.5 nm or 2-3 atomic layers

ESCA: electron spectroscopy for chemical analysis

- X-ray photoelectron spectroscopy (XPS)
- Auger electron spectroscopy (AES)
- Scanning Auger electron microscopy (SAM)

The photo effect (Albert Einstein 1905)

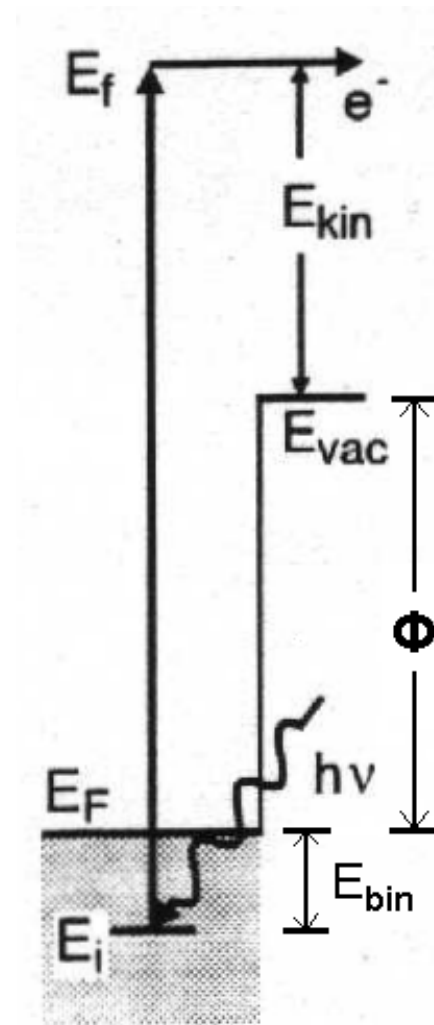


$$h \cdot \nu = E_{kin} + \Phi + E_{bin}$$

$$E_{kin} = h \cdot \nu - \Phi - E_{bin}$$

Φ : work function of the material (2 – 66 eV)

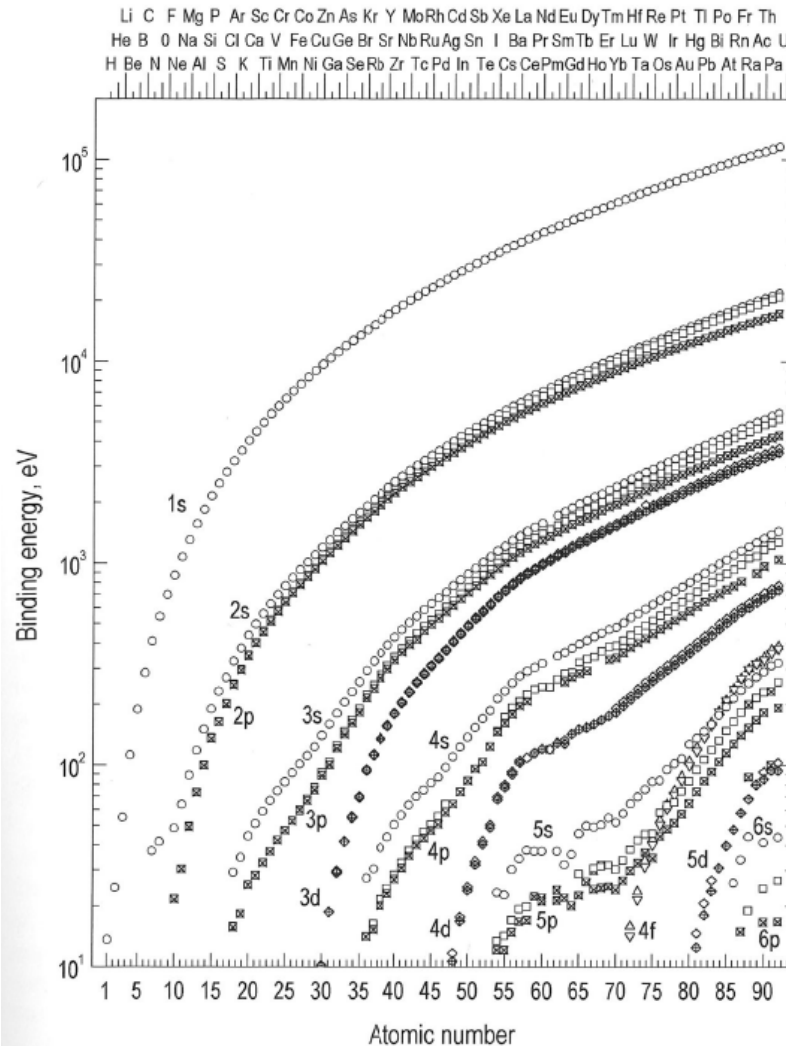
Measurement of $E_{kin} \rightarrow$ determination of binding energies of electrons in solids



Photoelectron spectroscopy

- **X-ray photoelectron spectroscopy (XPS):**
electron emission from atomic core level electron states ($50 \text{ eV} < h\nu$, (soft) X-rays)
- **Ultraviolet photoelectron spectroscopy (UPS):**
valence band electron states ($h\nu < 50 \text{ eV}$, excitation typically with (hard) UV-light)

X-ray photoelectron spectroscopy (XPS): core level energies

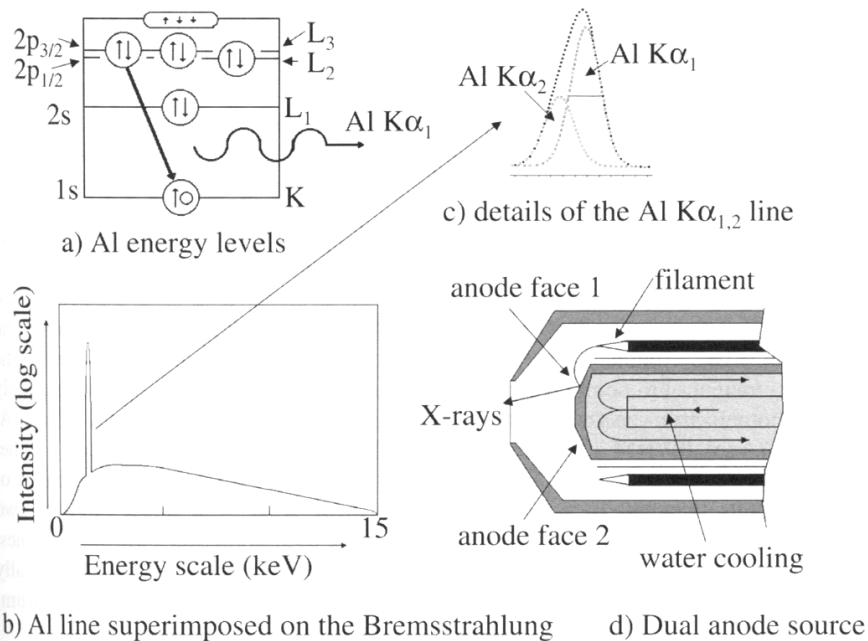


K. Oura et al.: Surface Science – An Introduction, Springer 2003

Laboratory photon sources for XPS I: basic elements

Laboratory-scale X-ray source: X-ray tube, K_{α} -radiation from **Al or Mg X-ray anode** material:

- Anode material is bombarded with high-energy (~ 15 keV) electrons
- The rapidly decelerated electrons generate a broad-band continuum of X-ray radiation of high photon energy rather non-specific of the anode material: **Bremsstrahlung**
- **Characteristic radiation:** narrow-band X-ray fluorescence caused by element-specific electronic transition in the anode material after impact ionization and generation of a **core hole** in the K shell
- Suppression of Bremsstrahlung by a thin Al window at the exit of the X-ray tube
- **Synchrotron radiation** is an important source of X-ray radiation with a continuous energy spectrum



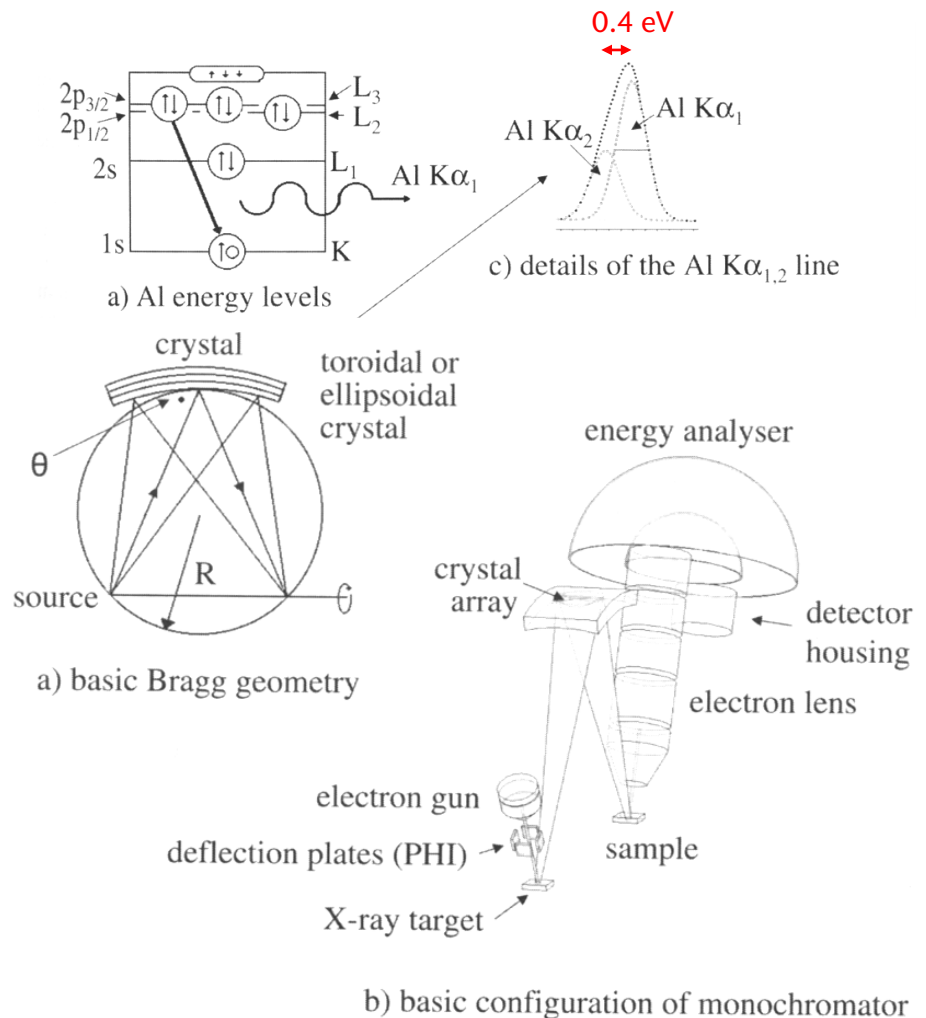
Source: Briggs, Grant: Surface Analysis by Auger and X-Ray Photoelectron Spectroscopy

$$\text{Al } K_{\alpha}: h\nu = 1.486,6 \text{ eV}$$

$$\text{Mg } K_{\alpha}: h\nu = 1.253,6 \text{ eV}$$

Laboratory photon sources for XPS II: X-ray monochromator

- **Broadening** of K_{α} lines by fine structure of core levels
 - Improvement of X-ray emission line width by X-ray monochromators to better than 0.3 eV
 - Deflectable electron beam allows to **rasterize the sample** with lateral resolution in the range of few micrometer („scanning photoelectron spectroscopy“)

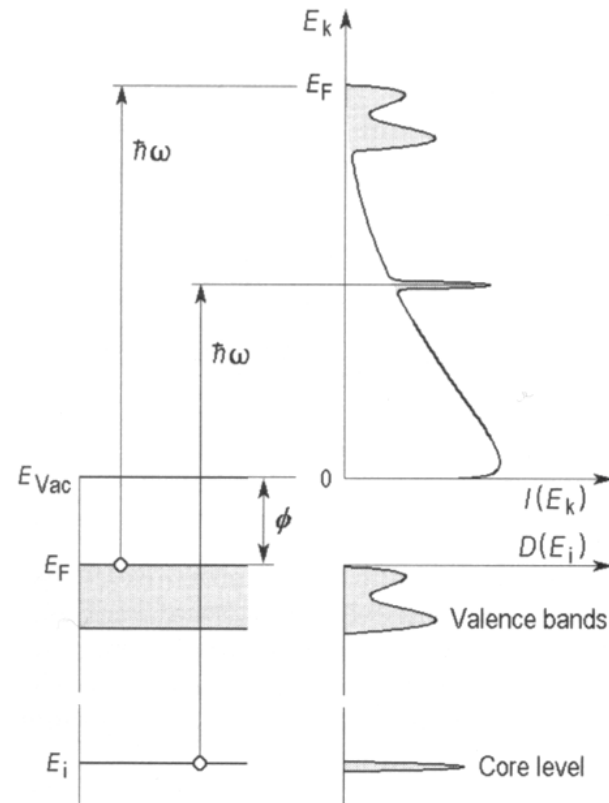


XPS: core level and valence band emission

- Binding energy versus kinetic energy
 - Binding energy of electrons in materials specified with respect to the Fermi level
 - Kinetic energy of photoelectrons just outside of the sample surface:

$$E_{kin} = \hbar\omega - E_i - \phi$$

$\hbar\omega$: photon energy
 E_i : binding energy of
 ϕ : work function of the material (depends on crystallographic surface orientation and a possible surface adlayer)
 - Background from inelastically scattered electrons at smaller kinetic energies than the photoelectron energy



K. Oura et al.: Surface Science – An Introduction, Springer 2003

X-ray photoemission spectroscopy (XPS): example spectrum

- Example: XPS spectrum of Ag

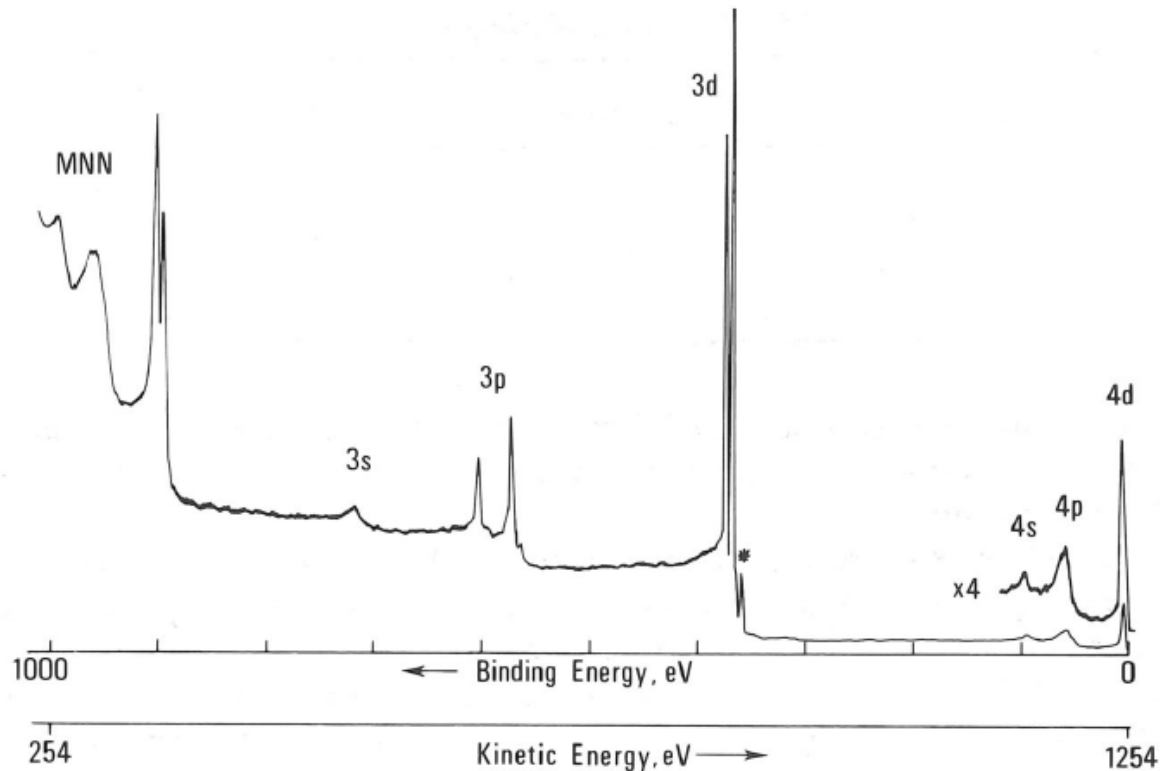


Figure 3.16 X-ray photo-electron spectrum of silver excited by Mg $K\alpha$ (essentially Mg $K\alpha_{1,2}$) and recorded with a constant analyser energy of 100 eV (*Ag 3d 'satellite' excited by Mg $K\alpha_{3,4}$)

Briggs, Grant: Surface Analysis by Auger and X-Ray Photoelectron Spectroscopy

X-ray photoemission spectroscopy (XPS): example spectrum

Satellites of photoelectron lines
from unmonochromatized X-ray
source

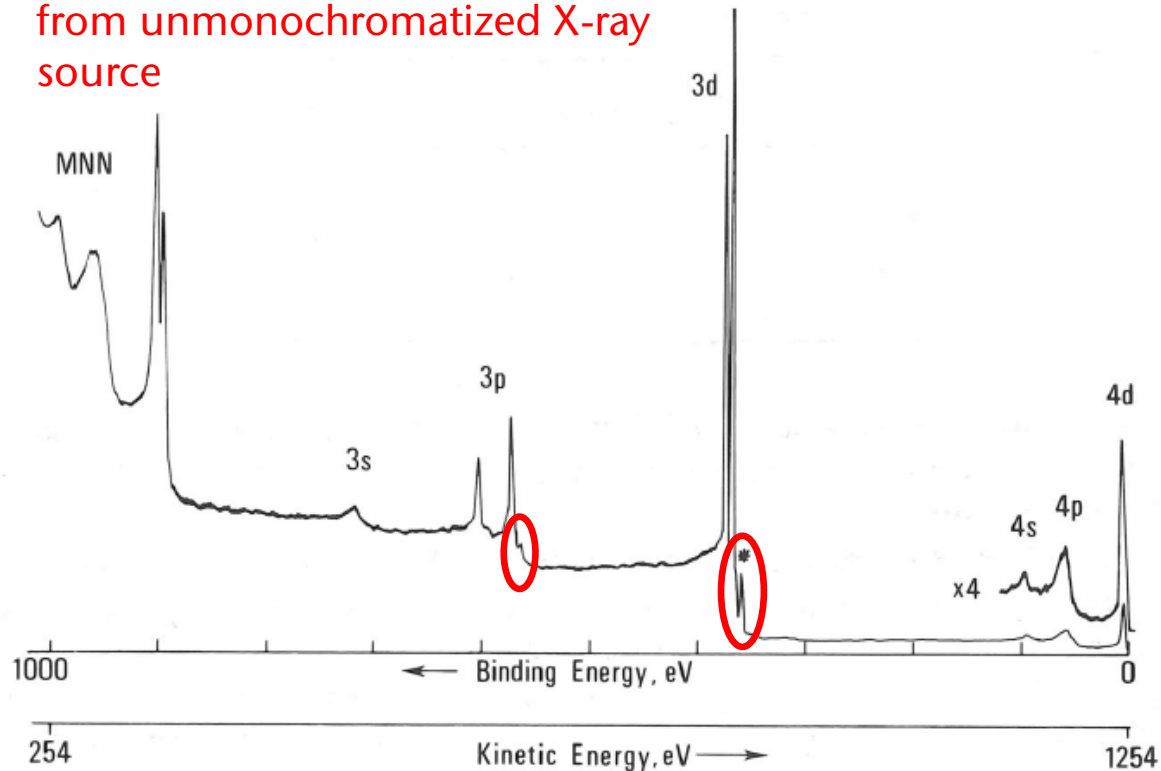


Figure 3.16 X-ray photo-electron spectrum of silver excited by Mg $K\alpha$ (essentially Mg $K\alpha_{1,2}$) and recorded with a constant analyser energy of 100 eV (*Ag 3d 'satellite' excited by Mg $K\alpha_{3,4}$)

Briggs, Grant: Surface Analysis by Auger and X-Ray Photoelectron Spectroscopy

X-ray photoemission spectroscopy (XPS): example spectrum

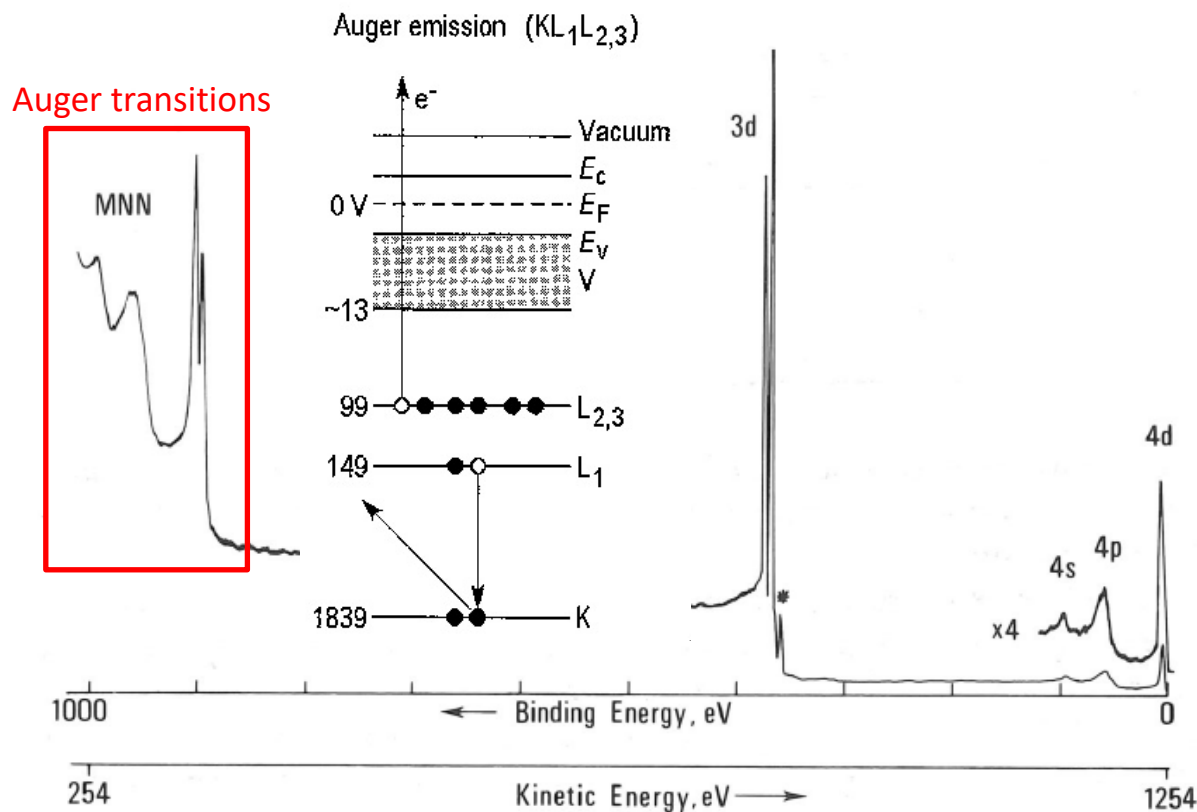


Figure 3.16 X-ray photo-electron spectrum of silver excited by Mg K α (essentially Mg K $\alpha_{1,2}$) and recorded with a constant analyser energy of 100 eV (*Ag 3d 'satellite' excited by Mg K $\alpha_{3,4}$)

X-ray photoemission spectroscopy (XPS): example spectrum

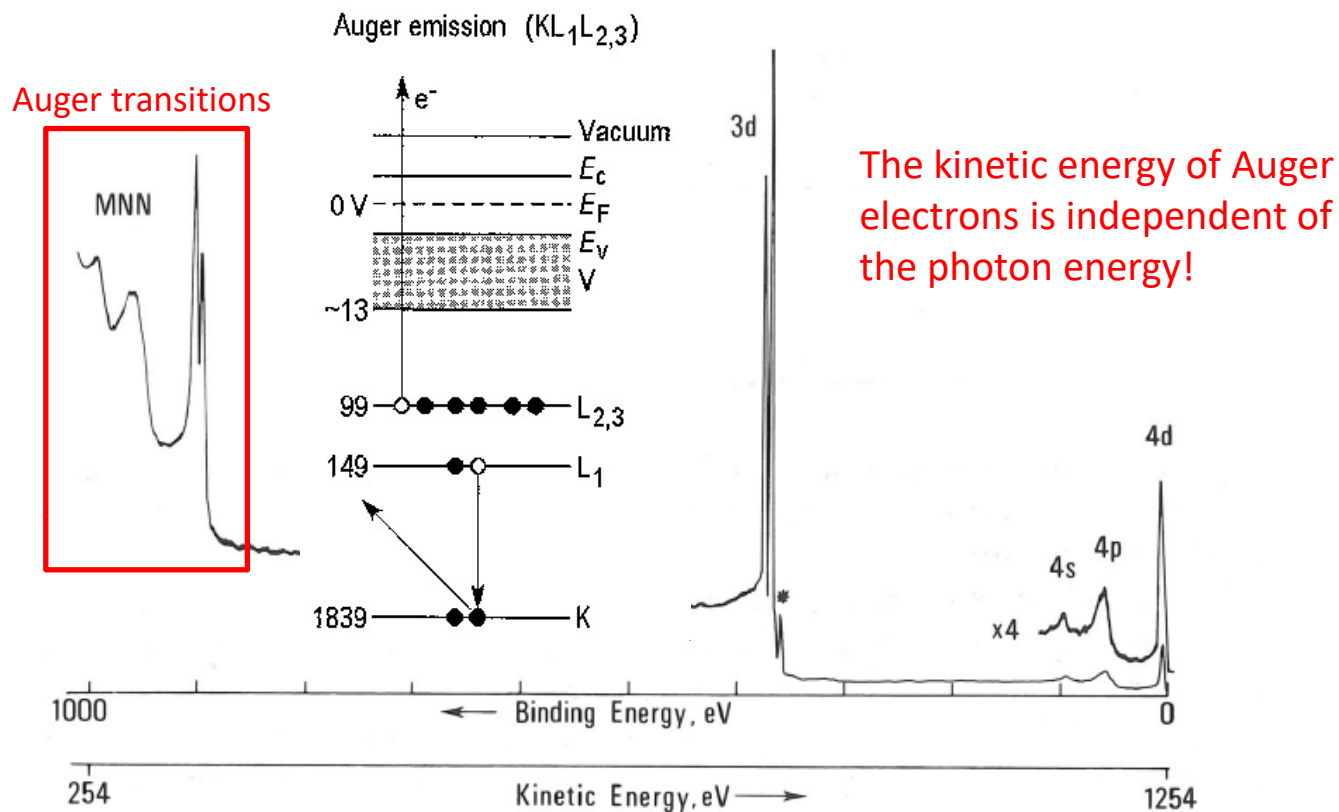
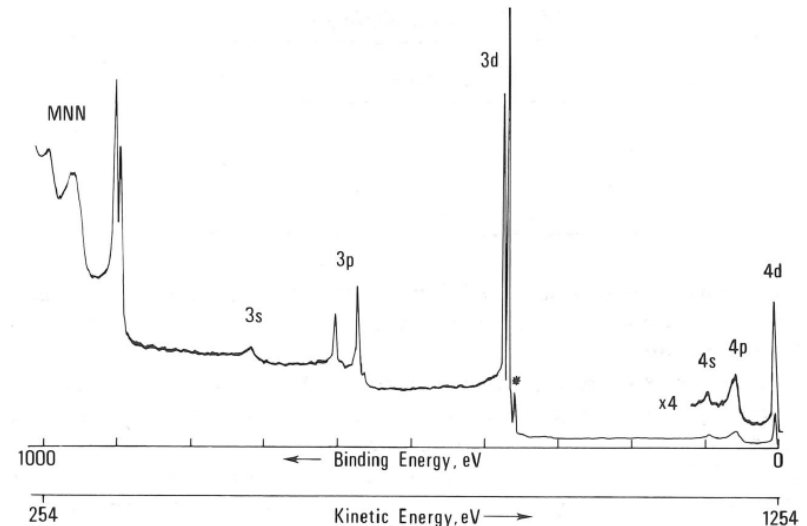


Figure 3.16 X-ray photo-electron spectrum of silver excited by Mg $K\alpha$ (essentially Mg $K\alpha_{1,2}$) and recorded with a constant analyser energy of 100 eV (*Ag 3d 'satellite' excited by Mg $K\alpha_{3,4}$)

Summary: structure of X-ray photoelectron spectra

- Characteristic lines from core level emission (valence band emission, although weaker, also present in the spectra)
- Presence of Auger lines (E_{kin} independent of photon energy \rightarrow discrimination from photoemission lines by variation of $\hbar\omega$ ermöglicht Unterscheidung)
- Non-monochromatized X-ray excitation:

Apperance of satellites at smaller binding energy (higher kinetic energy) caused by additional X-ray lines at higher energy



Briggs, Grant: Surface Analysis by Auger and X-Ray Photoelectron Spectroscopy

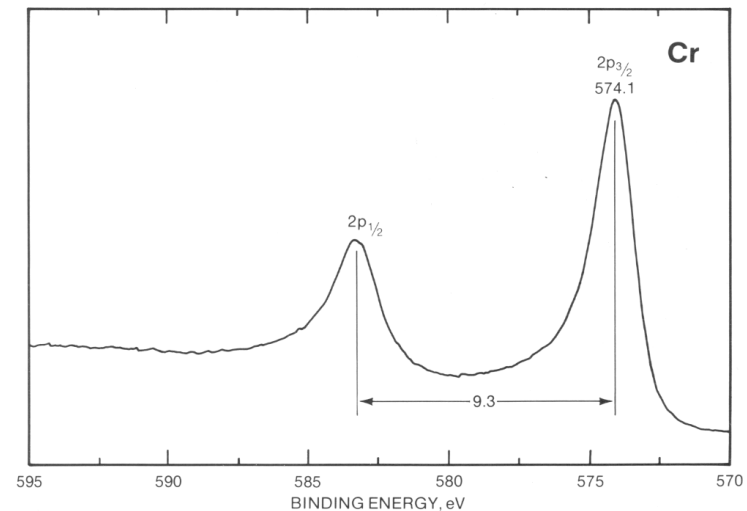
Source	Energy [eV]	Relative intensity	Typical intensity at the sample [photons/s]	Linewidth [meV]
MgK $_{\alpha 1,2}$	1253.6	100	$1 \cdot 10^{12}$	680
Satellites K $_{\alpha 3}$	1262.1	9		
K $_{\alpha 4}$	1263.7	5		
AlK $_{\alpha 1,2}$	1486.6	100	$1 \cdot 10^{12}$	830
Satellites K $_{\alpha 3}$	1496.3	7		
K $_{\alpha 4}$	1498.3	3		

M. O. Krause and J. G. Ferreira 1975,
J. Phys. B: Atom. Mol. Phys. 8 2007

Significance of spin-orbit coupling in photoelectron spectra

▪ **Spin-orbit coupling** (ls-coupling)

- Binding energy of electrons in atoms depend on the **total** angular momentum j of the electron
- Orbital momentum (l) and electron spin (s) add to the total angular momentum (j). Parallel and antiparallel orientation is possible: **splitting** of photoemission lines into **doublets**
- Relative integrated intensities of the doublet peaks correspond to the **degeneracy of the energy level**.



XPS handbook, Perkin-Elmer

- For example: $l = 1$ (p electrons)

quantum number of total angular momentum: $j = \left| l \pm \frac{1}{2} \right| = \frac{1}{2}, \frac{3}{2}$

magnetic quantum number $m_j = -j, \dots, j$ allows for $(2j + 1)$ possible orientations of \vec{j}

$j = \frac{1}{2}$: 2 possibilities $m_j = -\frac{1}{2}, +\frac{1}{2}$

$j = \frac{3}{2}$: 4 possibilities $m_j = -\frac{3}{2}, -\frac{1}{2}, +\frac{1}{2}, +\frac{3}{2}$

-> intensity ratio 1:2

- For s electrons ($l = 0$) only $j = \frac{1}{2}$ possible -> no spin-orbit splitting

Many-particle effects in XPS

- Binding energies: single particle description vs. many-particle description
 - Up to now: only non-interacting electrons considered (single-particle picture)
 - Often can this picture be used to a good approximation, but larger deviations observed for example for rare earth metals
 - More realistic description: an atom with N electrons becomes an (ionized) atom with $(N - 1)$ electrons after photoemission
 - „Shake-Up“ satellites:
 - After removal of a core electron (generation of a „core hole“) the valence electrons „see“ Entfernen eines Rumpfelektrons „sehen“ Valenzelektronen erhöhte Kernladungszahl
 - Energetic reorganisation of the valence electrons (relaxation) into states with higher binding energy
 - Kinetic energy of the emitted photoelectron is reduced by this reorganisation energy

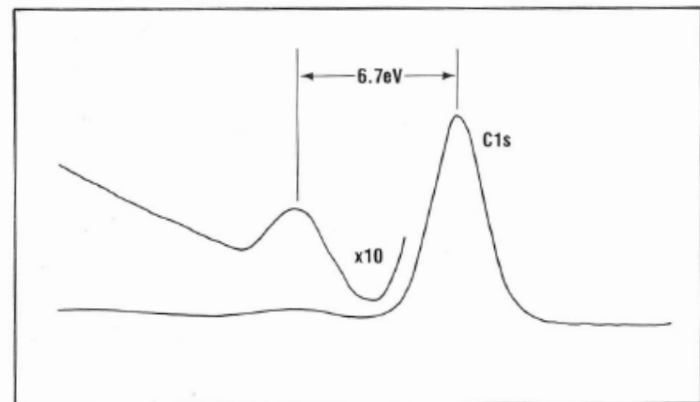
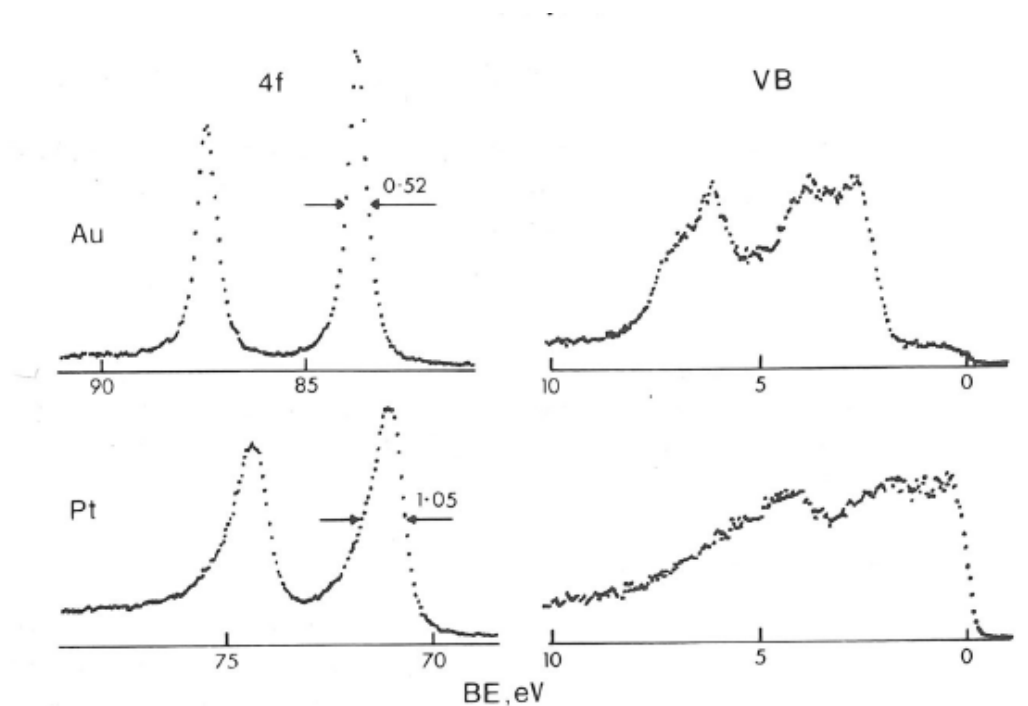


Figure 7. The π -bond shake-up satellite for the C1s line in polystyrene.

XPS Handbook, Perkin-Elmer

Shake-up effects in XPS lines of metals

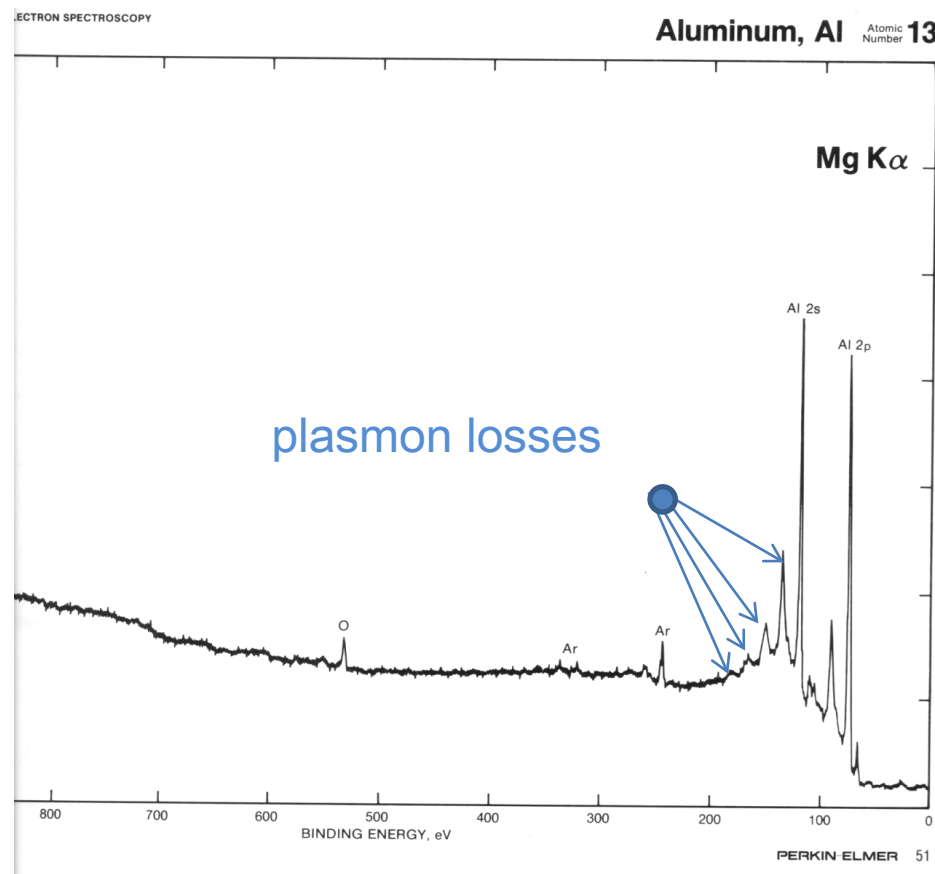
- Asymmetrically broadened XPS line shapes in metals caused by „shake-up“ processes in the continuum of states near the Fermi level



Briggs, Grant: Surface Analysis by Auger and X-Ray Photoelectron Spectroscopy

More spectral features in XPS: plasmon losses

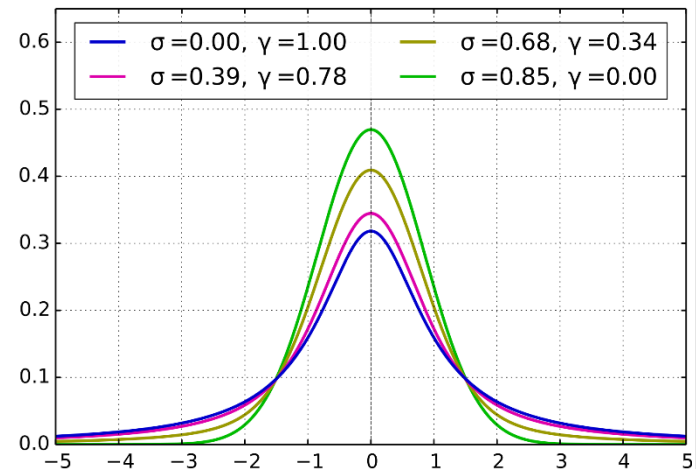
- **Equidistant energy loss peaks** of photoelectrons caused by excitation of collective motion of conduction electrons in metals, called **plasmons**



XPS Handbook, Perkin-Elmer

Quantitative analysis of XP spectra I

- XPS can be used for the quantitative analysis of the **relative concentration of chemical elements** in the near-surface region of the material
- For that purpose, the **integrated intensity of the photoemission lines** have to be determined by fitting of model functions to the measured spectra.
- Measured line width: $\Delta E = \sqrt{\Delta E_n^2 + \Delta E_p^2 + \Delta E_a^2}$
 ΔE_n : natural line width of the photoemission line,
 ΔE_p : line width of the X-ray radiation
 ΔE_a : energy resolution of the energy analyzer
 $(\Delta E_n \ll \Delta E_p \text{ for non-monochromatized X-ray sources})$
- **Modeling of XPS peaks by Voigt profiles:**
 convolution of a Lorentz profile (spectral profile of photo excitation) with a Gauß profile
 (instrumental profile for finite energy resolution of the energy analyzer)



https://commons.wikimedia.org/wiki/File:Mplwp_Voigt-HWHM1.svg

$$f_G(\omega, \sigma) = e^{-\frac{(\omega - \omega_0)^2}{2\sigma^2}}$$

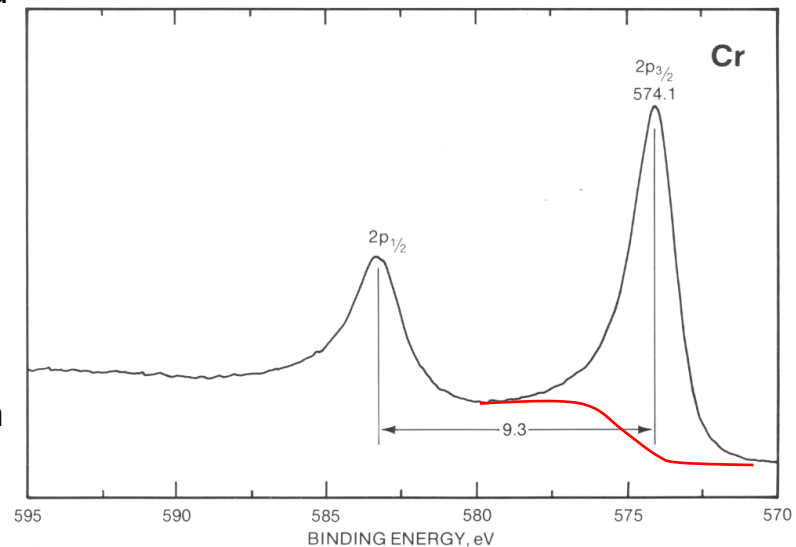
$$f_L(\omega, \gamma) = \frac{1}{(\omega^2 - \omega_0^2)^2 + \omega_0^2 \cdot \gamma^2}$$

$$f_V(\omega, \sigma, \gamma) = \int f_G(\tau) f_L(\omega - \tau) d\tau$$

Quantitative analysis of XP spectra II

- Line shape can be asymmetrically broadened by loss processes such as „shake-up“ processes in metals
- Close to a photoemission line the background has a step-like shape (**red line**) on account of a step-like increase of inelastically scattered secondary electrons
- For quantitative analysis of integrated peak intensities a suitable background subtraction must be performed:
 - Shirley background: the additional background $S(E)$ generated by photoelectrons assignable to photoelectron peak $P(E)$ is proportional to the integrated photoelectron intensity of that peak for energies $> E$:

$$S(E) = k \cdot \int_E^{+\infty} P(E') dE'$$
 - There are other models for background description and subtraction



XPS Handbook, Perkin-Elmer

XPS for quantitative analysis of surface concentrations I

- Quantification of relative concentration using sensitivity factors derived from
 - reference measurements of relative intensities of various XPS lines from neat samples of polished surface quality if possible.
 - The intensity of a specific elemental XPS line (F 1s, for example) is chosen as the reference. The intensities of all other photoemission lines are referred to this intensity value.
 - **Sensitivity factors** are defined by

$$S_k = \frac{I_k^\infty}{I_{Ref}^\infty}$$

I_{Ref}^∞ : intensity of the reference (∞ denotes thick, bulk-like sample)

I_k^∞ : intensity of a bulk-like sample of material k

XPS for quantitative analysis of surface concentrations II

- Elemental concentration can then be calculated using the formula:

$$c_A = \frac{I_A/S_A}{\sum_{k=A,B,\dots} I_k/S_k}$$

I_X : intensity of a characteristic XP peak of element X

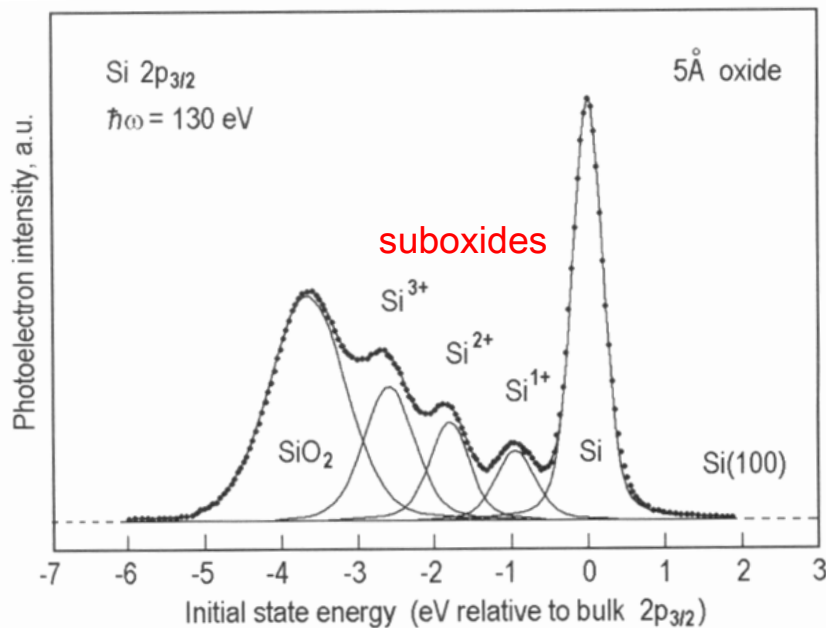
S_X : sensitivity factor of the XP peak of element X

index k numbers all elements present at the surface

- Application of this formula implies a homogeneous spatial distribution of the chemical elements in the material. If this is not the case, a suitable model for the spatial distribution of the elements must be established and compared with the experimental data.

XPS for characterization of chemical bonds near the surface I

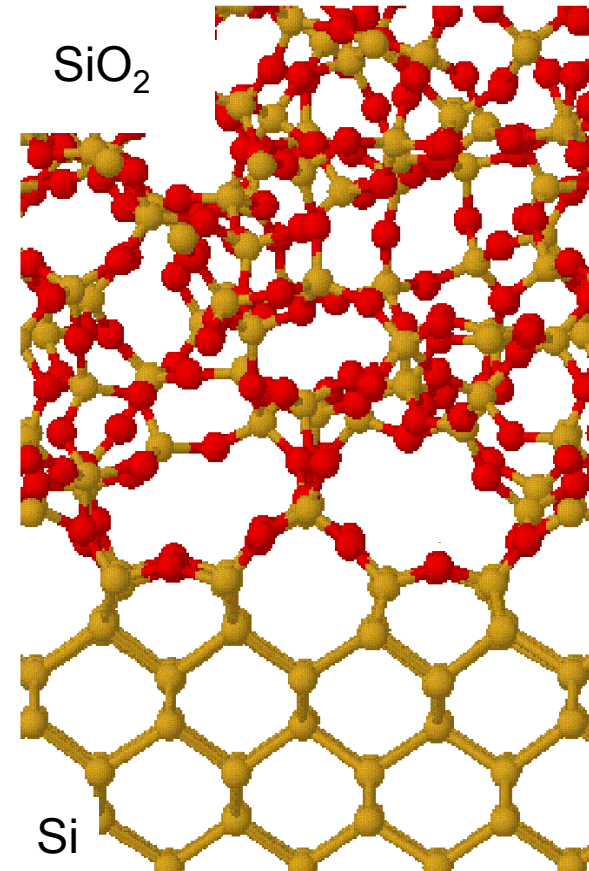
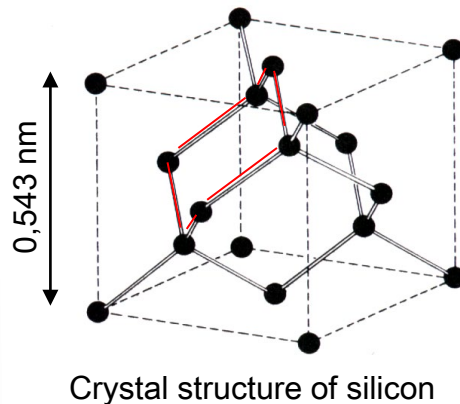
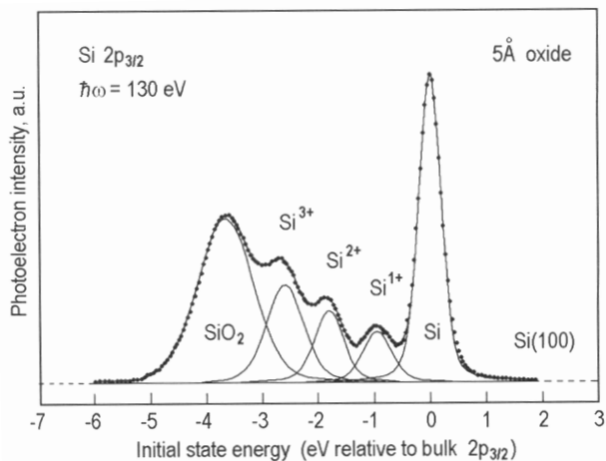
- **Chemical shifts** of photoemission lines
 - Observation of energy shifts of binding energies in chemical compounds
 - Example: **Si(100) single crystal surface** (wafer) covered with a 0.5 nm thin layer of native SiO_2



- Charge transfer upon formation of Si-O bonds
- Change (increase) of binding energy of core level electrons by changed (reduced) screening of nuclear charge
- Amount of chemical shift depends on the electronegativities of the involved elements
- Chemical shift results in different energetic positions of the $\text{Si } 2p_{3/2}$ peaks depending on the oxidation level (contribution of $2p_{1/2}$ peak in the doublet has been subtracted)

F. J. Himpsel et al., Phys. Rev. B **38** 6084 (1988)

XPS for characterization of chemical bonds near the surface II

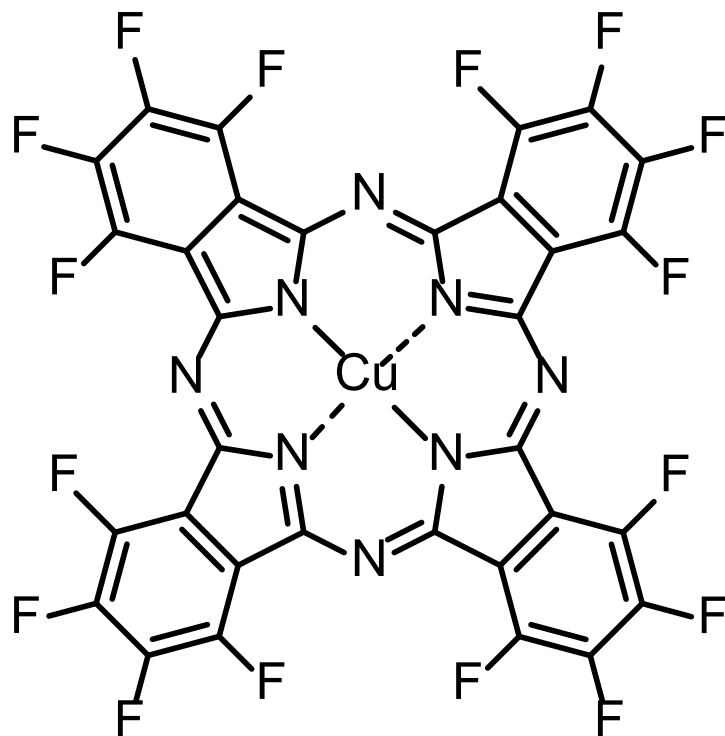


Yu, Tersoff, Phys. Rev. Lett 84 (2000), 4393

An ideal, atomically flat Si(100)-SiO₂ system should have only oxidation levels 0, 2+ and 4+!

The presence of oxidation levels 1+ and 3+ in real Si(100)-SiO₂ systems indicates atomic roughness of this interface.

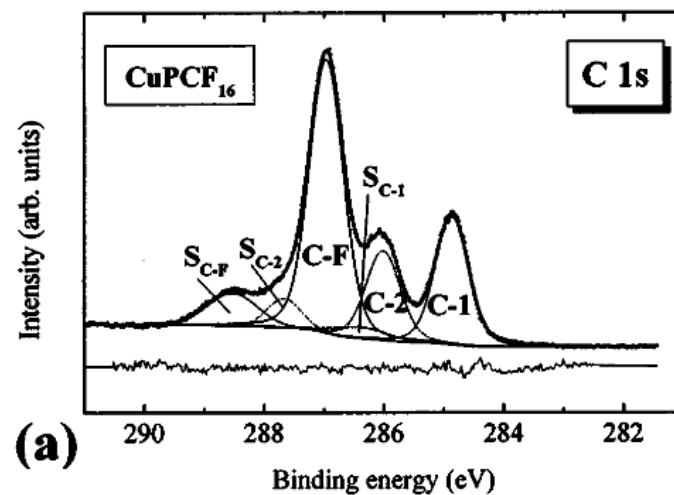
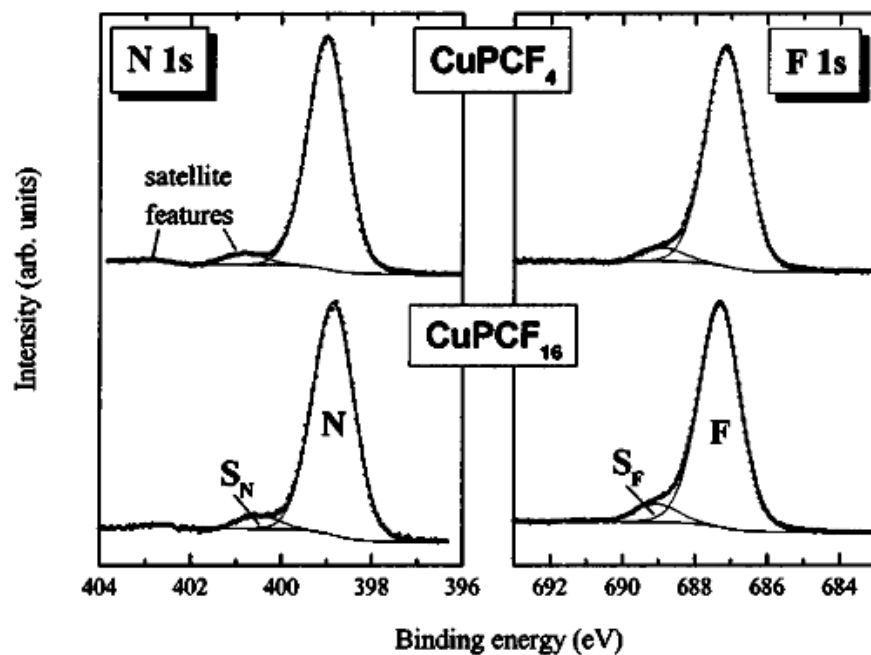
$F_{16}CuPc$ – copper-hexadecafluorophthalocyanine studied as thin film in the lab exercise



Lab exercise: XPS of $F_{16}CuPc$ on SiO_2

- Sample consists of several layers $F_{16}CuPc$ on SiO_2
- Measure full XPS spectrum and C 1s detailed spectrum
- Calibrate energy axis using the F 1s emission line. Determine the energy resolution of the experiment
- Assign the bands of the full spectrum to chemical species. Use both X-ray anodes to discriminate Auger lines from photoemission lines
- Analyze the photoemission components of the C 1s spectrum and explain their origin

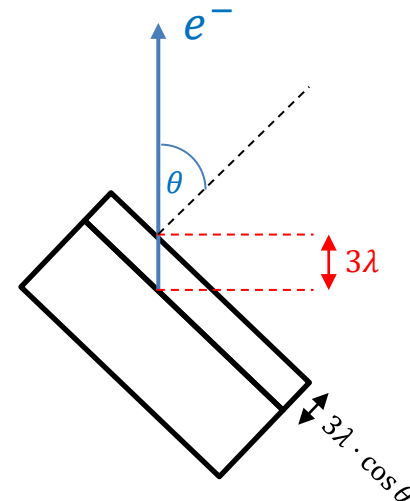
XPS of $F_{16}CuPc$



H. Peisert et al., J. Appl. Phys. 93 (2003), 12, 9683-9692.

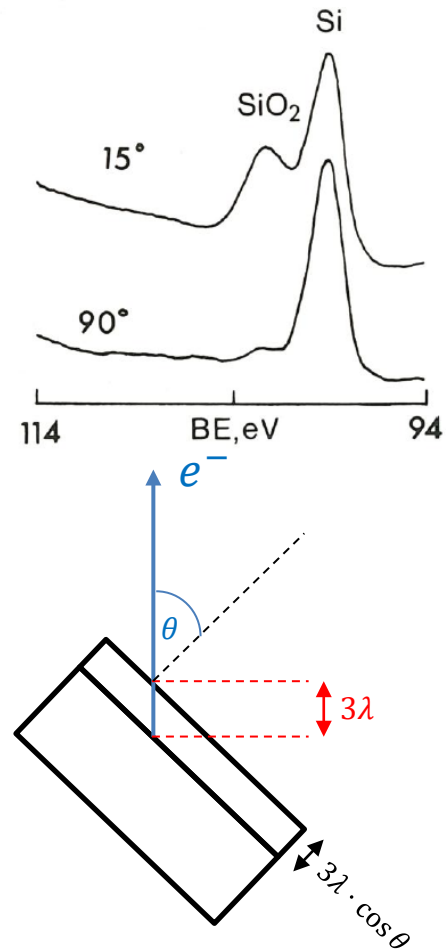
Exploiting the energy dependence of the escape depth in XPS I

- Angle dependence of photoemission
 - Increase the surface sensitivity of XPS by grazing incidence
 - Photoelectron signal from distance d below the surface is exponentially damped by the material
 above: $I(d) = I_0 e^{-\frac{d}{\lambda}}$
 λ : mean free path
 - 95% of the photoelectrons originate from a 3λ -deep region below the surface
 - Changing the emission angle changes the ratio of surface-to-bulk contribution of the photoemission signal.



Exploiting the energy dependence of the escape depth in XPS II

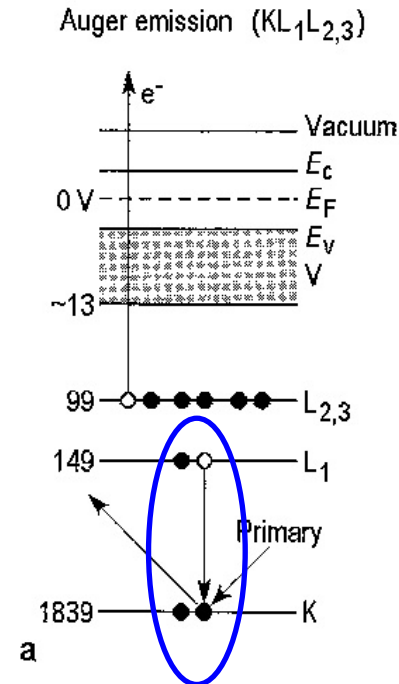
- Angle dependence of photoemission
 - Increase the surface sensitivity of XPS by grazing incidence
 - Photoelectron signal from distance d below the surface is exponentially damped by the material
above: $I(d) = I_0 e^{-\frac{d}{\lambda}}$
 λ : mean free path
 - 95 % of the photoelectrons originate from a 3λ -deep region below the surface
 - Changing the emission angle changes the ratio of surface-to-bulk contribution of the photoemission signal.



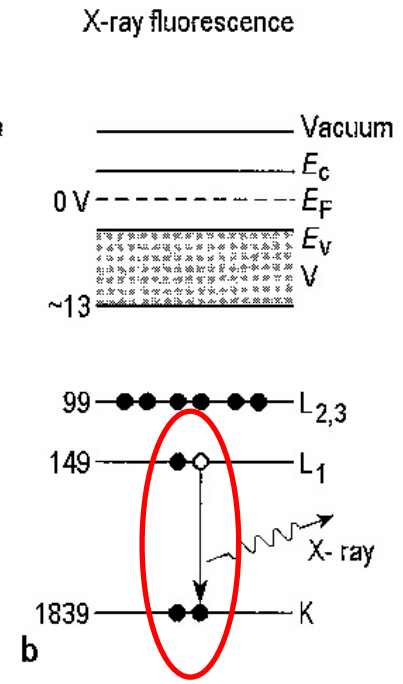
Auger electron spectroscopy (AES)

Oura: Surface Science

- Generation of a **core level hole** by impact ionization caused by electron bombardment or by X-ray ionization. Highly excited state, hole is filled by electron from a higher level.
- Excess energy in this process can be released as X-ray quantum of X-ray fluorescence or **radiationless** by emission of a second electron of the atom.
- The second process is called **Auger process** (named after the French physicist Pierre Auger who discovered this effect around 1920)
- The atomic Auger process is a 3-electron-process: Auger process is not possible in H or He!



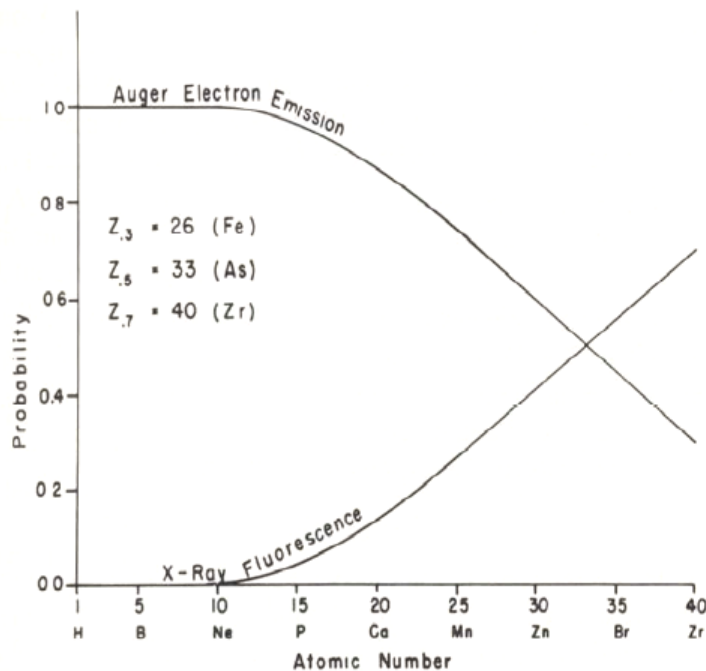
$KL_1L_{2,3}$ Auger emission is possible



This radiative process is dipole-forbidden ($\Delta l = 0$)!

Auger emission versus X-ray fluorescence

Probability of Auger emission and X-ray fluorescence following ionisation of a K-shell electron:



The Auger process dominates for small atomic numbers Z ($Z > 2$) over X-ray fluorescence. For $Z > 34$ X-ray fluorescence prevails.

X-ray fluorescence following K-shell ionization possible only for atoms with $Z > 4$, starting with boron. Occupation of at least 2p electron states required.

Abb. 3.8: Relative probabilities of relaxation by emission of an Auger electron and by emission of an X-ray photon of characteristic energy, following creation of a core hole in the K shell

Briggs, Grant: Surface Analysis by Auger and X-Ray Photoelectron Spectroscopy

Quantum mechanical basis of AES transitions

- Transition probability and selection rules
 - Energy transfer between the electrons in the atom is mainly controlled by **Coulomb interaction**.

- Coulomb interaction energy between two electrons at positions \vec{r}_1 and \vec{r}_2 :

$$V_{WW}(\vec{r}_1, \vec{r}_2) = \frac{e^2}{4\pi\epsilon_0 |\vec{r}_1 - \vec{r}_2|}$$

- Transition probability of KLL process:

$$W_{KLL} \sim \int \psi_{1s}^*(\vec{r}_1) e^{-i\vec{k} \cdot \vec{r}_2} \frac{e^2}{|\vec{r}_1 - \vec{r}_2|} \psi_{2s}(\vec{r}_1) \psi_{2p}(\vec{r}_2) d^3r_1 d^3r_2$$

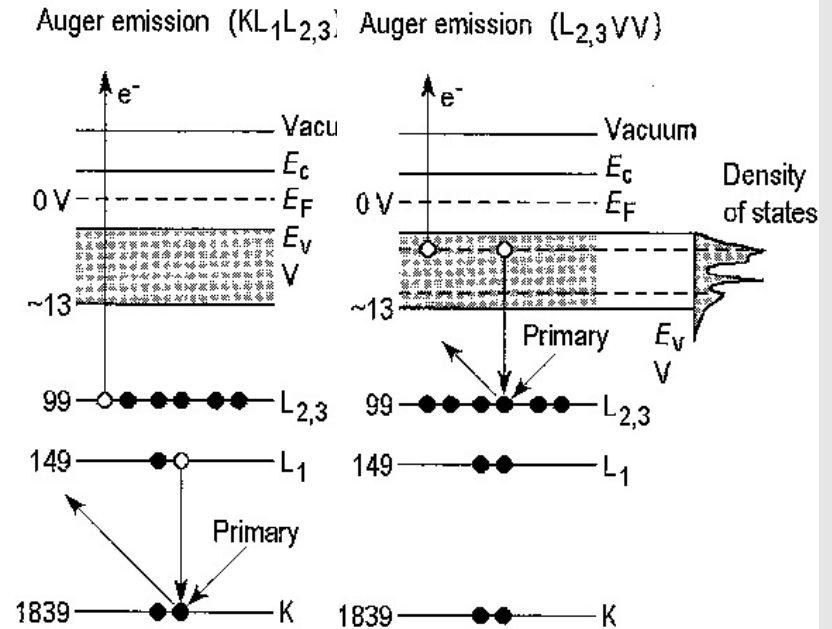
- Initial state in example above: two electrons, one in 2s and the other in 2p state
- Final state: one electron filling the core hole is in the ground state, another electron leaves the atom as a freely propagating plane electron wave (= Auger electron).
- Auger transitions do **not** obey dipole selection rules ($\Delta l = \pm 1, \Delta m_l = 0, \pm 1$) of optical transitions.

Auger processes in solids

- Assuming that the generation of a core hole in the atom does not perturb the energies of the other electrons, the **kinetic energy** of the Auger electron is given by

$$E_{KL_1L_{2,3}} = E_K - E_{L_1} - E_{L_{2,3}} - \phi$$

and independent of the energy of the core-hole generating electrons (typically $E > 2000$ eV) and of the X-ray photons.
- If valence band states are involved in the transition, they are denoted with „V“.
- Coarse above approximation of Auger electron energy falsely neglects reduced screening of the core hole and thus the higher binding energies of the other two electrons involved in the process.



Oura: Surface Science

Approximation for a correction of Auger energies

- After core hole generation, the residual Z-1 electrons interact with a nucleus with an effective atomic number between Z and Z+1
- Approximately corrected energies of electron in L_1 shell:

$$E_{L_1} = \frac{1}{2} (E_{L_1}^{Z+1} + E_{L_1}^Z)$$

- Approximated correction of Auger electron energy:

$$E_{KL_1L_{2,3}} = E_K - \frac{1}{2}E_{L_1}^Z - \frac{1}{2}E_{L_{2,3}}^Z - \frac{1}{2}E_{L_1}^{Z+1} - \frac{1}{2}E_{L_{2,3}}^{Z+1} - \phi$$

- More complicated correlation effects between the remaining electrons can still change actual Auger energies by several eV!

Chart and electron spectra of Auger transitions

- Energies of Auger transitions in dependence of atomic number

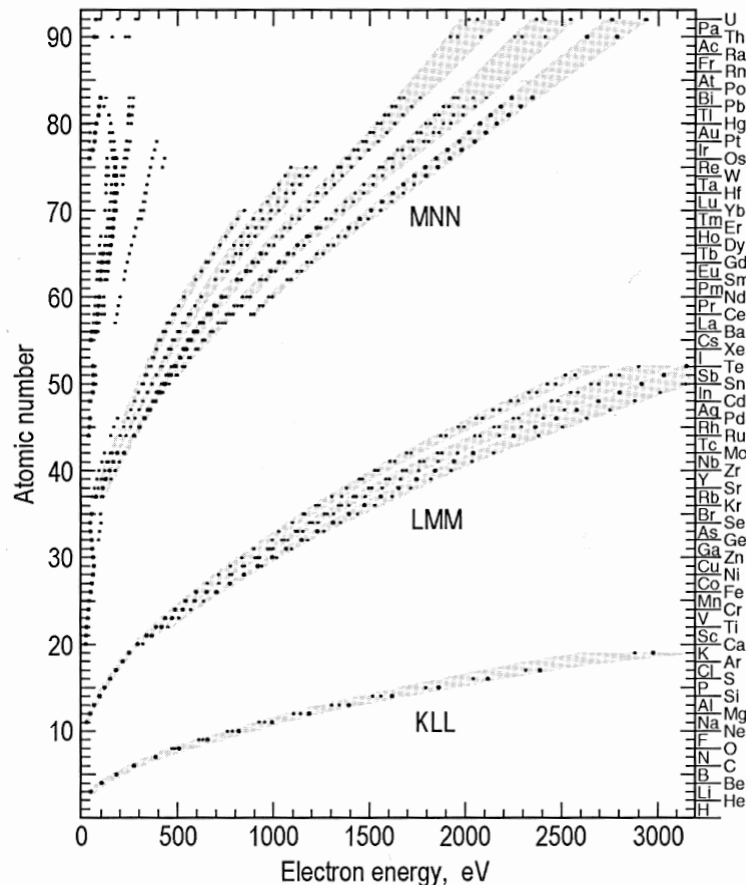


Fig. 5.8. The principal Auger electron energies for the elements used for qualita analysis. Three main series KLL, LMM and MNN are indicated. The dots indi the strongest and most characteristic peaks and the gray bands indicate the rc structure of less intense peaks [5.3]

Oura: Surface Science

Adjacent elements in the periodic system of elements often have similar spectra with moderately shifted Auger energies.

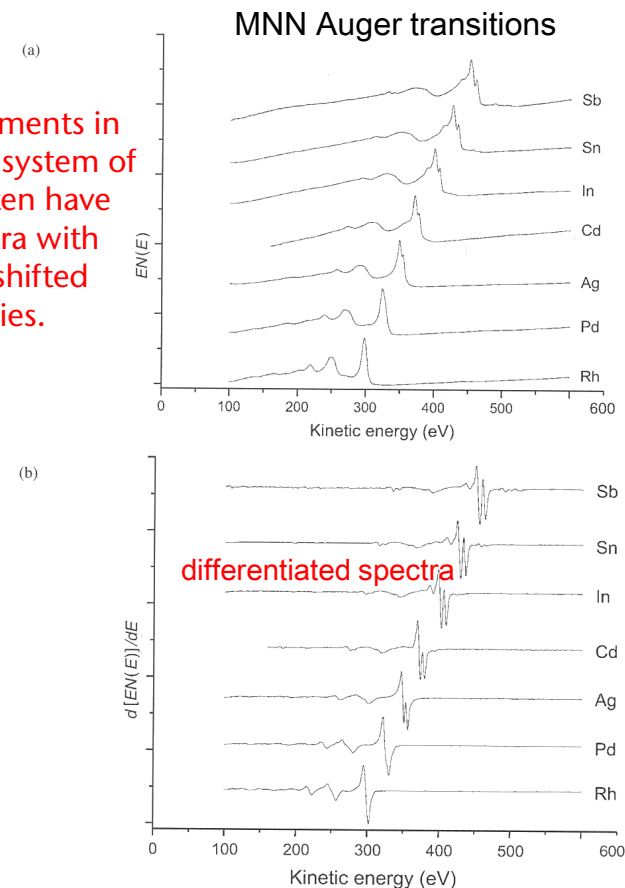
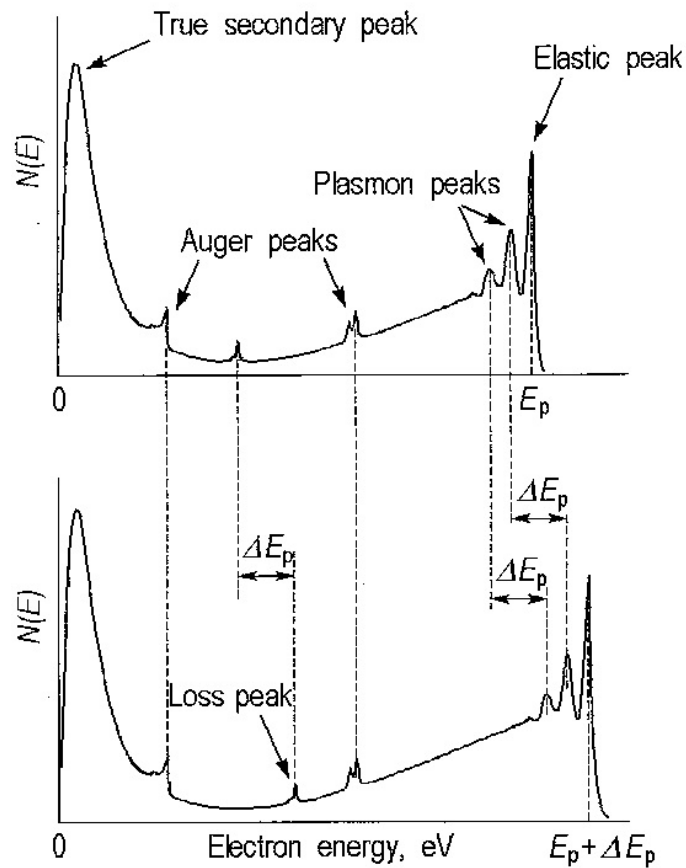


Figure 6. Auger spectra of Rh, Pd, Ag, Cd, In, Sn and Sb taken from argon-sputtered foils (except Cd was from CdS and Sb was from GaSb), (a) direct spectra taken with pulse counting and (b) derivative spectra taken in the computer. These spectra were obtained with a 10 nA, 5 keV electron beam and a hemispherical analyser with a 0.2 eV step interval. Spectra was taken in the FRR mode with an energy resolution of 0.6%. The spectra are offset for clarity.

Spectral features in Auger electron spectra



- Spectra dominated by elastically scattered primary electrons and secondary electrons („True Secondaries“ after many inelastic scattering processes)
- Electrons with material-specific, characteristic energy losses :
 - Excitation of plasmons, interband/intraband transitions, phonons, vibrations of adsorbed molecules etc.
 - Electron Energy Loss Spectroscopy (EELS, HREELS)
- Kinetic energies of Auger electrons independent of the energy of the core-hole-exciting electrons (primary electrons), as opposed to the kinetic energy of photoelectrons.

Efficiency of core-hole generation by electron impact

- Ionization cross sections for K hole generation

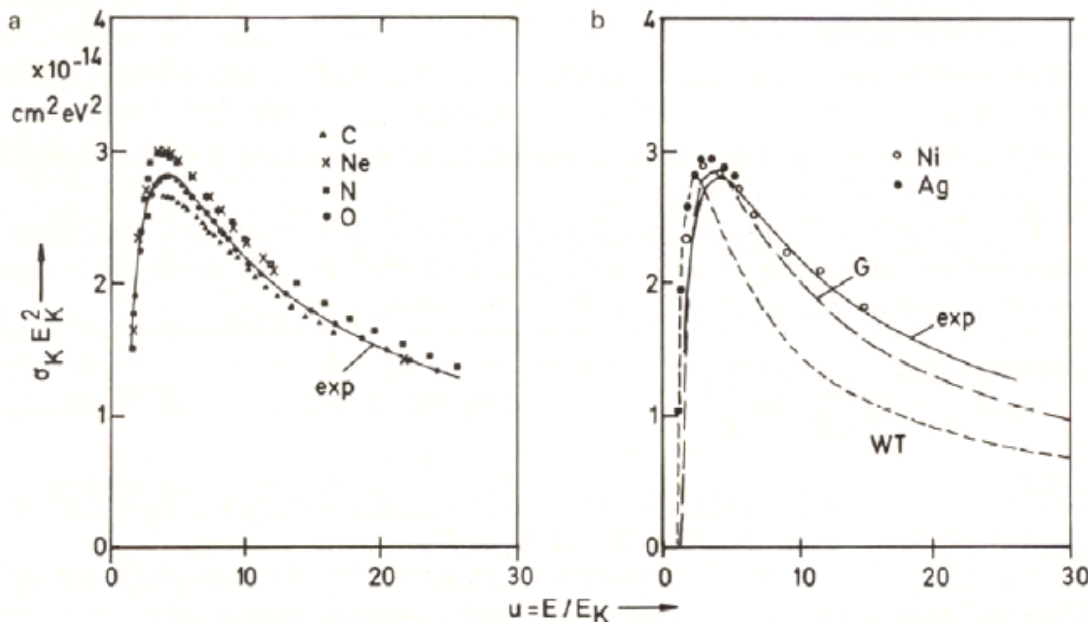


Abb. 3.5: Demonstration that the curve relating $\sigma_K E_K^2$ to the overvoltage ratio $u = E/E_K$ (σ_K = ionisation cross-section and E_K = ionisation energy of the K shell) is independent of atomic number. Experiments for (a) C, Ne, N and O atoms and (b) Ni and Ag atoms. Comparison with formulae of Worthington and Tomlin (WT) (3.84) and Gryzinski (G) (3.85) (see [3.31] for references)

Source: Reimer, Scanning Electron Microscopy, Springer 1985

E_K : threshold energy for ionization of K shell

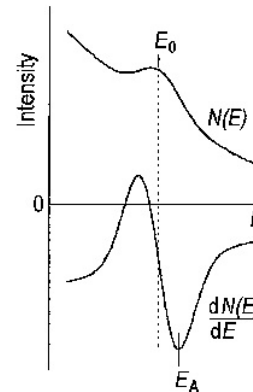
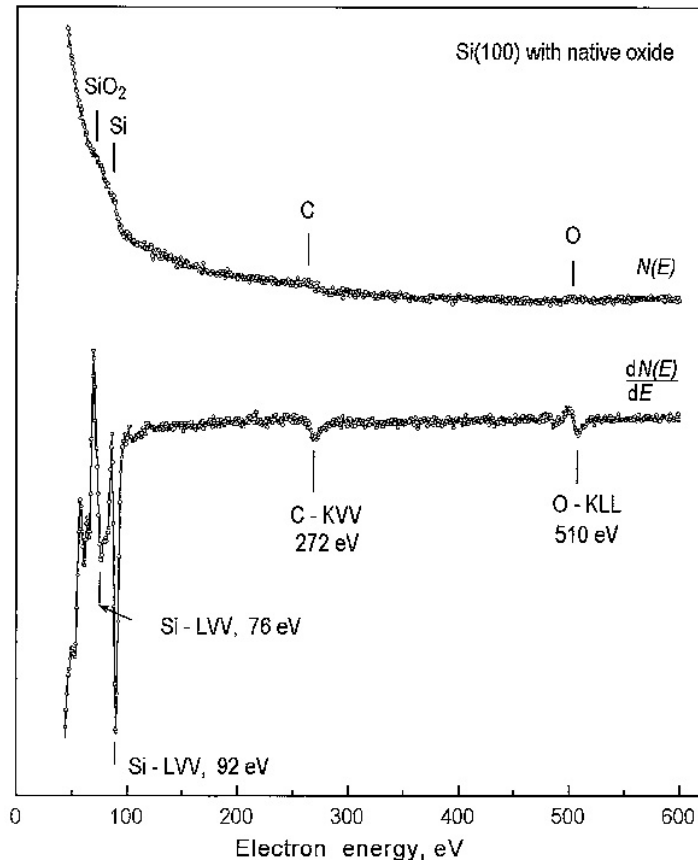
Maximum of ionization cross section is **independent of the material** about 3-times of the threshold energy

Formula for cross section of K shell ionization:

$$\sigma_K = \frac{\pi e^4 z_K b_k}{(4\pi\epsilon_0)^2 E_K^2} \frac{\ln u}{u}$$

z_K : Elektronen in der Schale
 $b_K \approx 0,35$
 $u = E/E_K$

Elimination of strong background effects by differentiation of Auger spectra

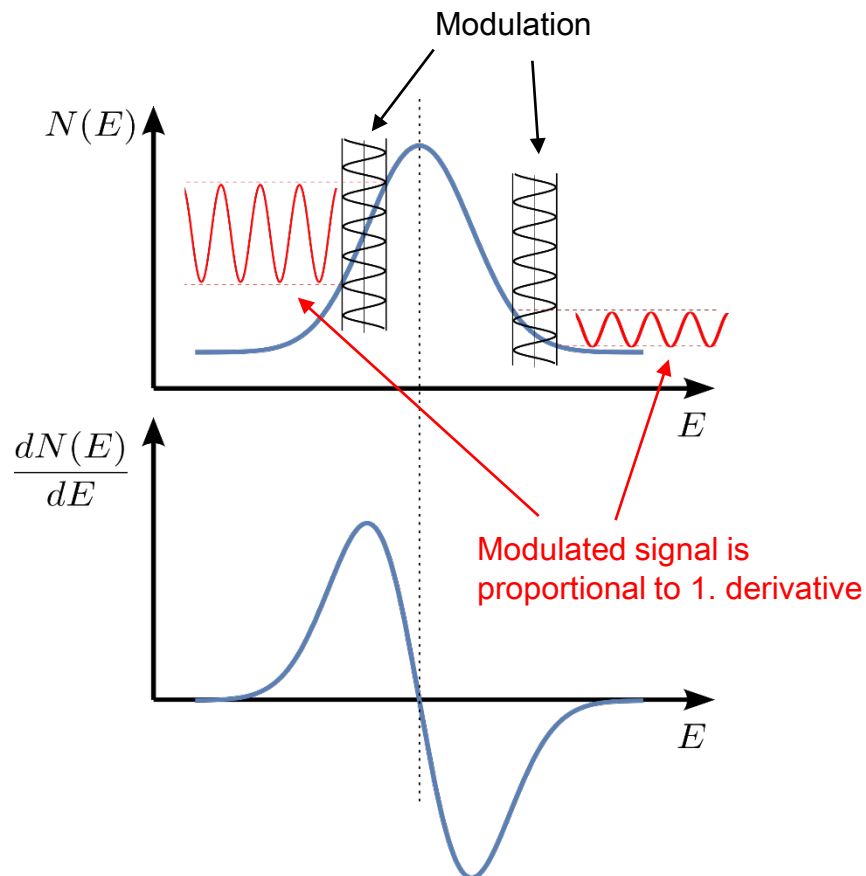
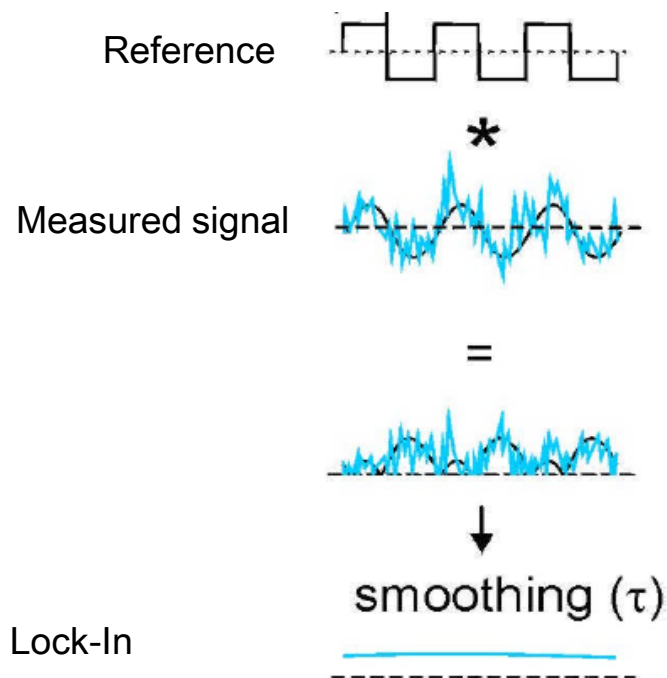


Energetic position of Auger lines are defined by the minimum of the differentiated spectrum

K. Oura et al.: Surface Science – An Introduction, Springer 2003

Differentiation of Auger electron spectra

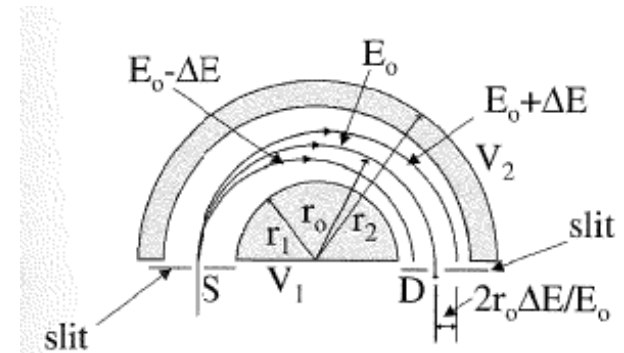
- Modulation method:
 - Lock-In amplifier
 - Signal/Noise ratio bis $S/N \sim 1/10.000$ possible



Energy detection of Auger and photoelectrons („energy filter“)

- We use a **hemispherical energy analyzer (HSA)**

- Deflection of electrons in the concentric electrostatic field between two spherical shells with potential difference $\Delta V = V_2 - V_1$
- Electrons with „**pass energy**“ $E_0 = e\Delta V \frac{R_1 R_2}{R_2 - R_1}$ move along a concentric circular path through the analyzer (bei senkrechtem Eintritt $\alpha = 0$)



Briggs, Grant: Surface Analysis by Auger and X-ray Photoelectron Spectroscopy

- Energy distribution of Auger and photoelectrons with width ΔE results in a distribution of the diameter of the circular paths with width $2r_0 \Delta E / E_0$
 - With finite width w of the exit slit, electrons pass the analyzer within an energy intervall $\Delta E = E_0 \frac{w}{2R_0}$ (band pass)

Operation modi of electrostatic energy analyzers

Constant pass energy – constant analyzer energy (CAE) / fixed analyzer transmission:

- ΔV and E_0 constant
- Constant energy resolution across the entire spectrum
- Best energy resolution at possibly lowest pass energy
- But analyzer transmission is low at high energy resolution Auflösungsvermögen
- By electron lenses electrons are decelerated / accelerated in front of the analyzer entrance for the correct pass energy
- Mainly used for PES / XPS

Constant retard ratio (CRR) oder fixed retard ratio (FRR)

- Pass energy E_0 is varied and, at the same time, electrons with original energy E are decelerated to keep $CRR = E_0/E$ constant
- Energy resolution becomes worse with increasing pass energy, but transmission increases
- Mainly used for AES
 - Higher sensitivity for weak Auger transitions at high energies
 - Avoids detector saturation at low energies (high background from secondary electrons)

Electron detection in AES and XPS/PES

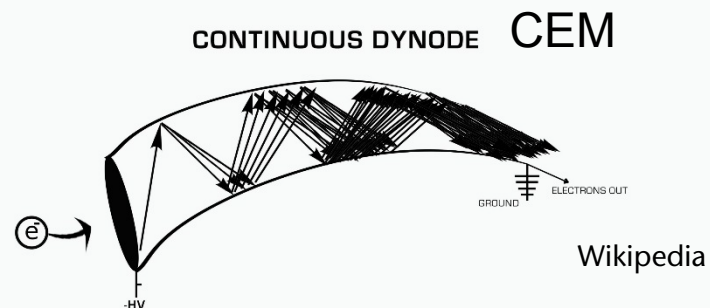
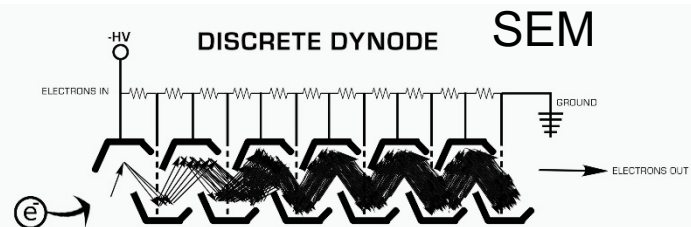
■ Electron detectors

Secondary electron multiplier – SEM

- Electrons are accelerated to discrete dynodes and excite 2-3 secondary electrons per impinging electron
- Avalanche effect by cascaded dynodes
- Total voltage ~ 2 kV
- Amplification up to 10^7

■ Channel electron multiplier – CEM, channeltron

- Similar to SEM, but continuous dynode
- Even voltage drop along the CEM glass wall covered with high-ohmic material
- Total voltage ~ 2 kV
- More compact device than SEM
- Amplification: $10^5 - 10^6$



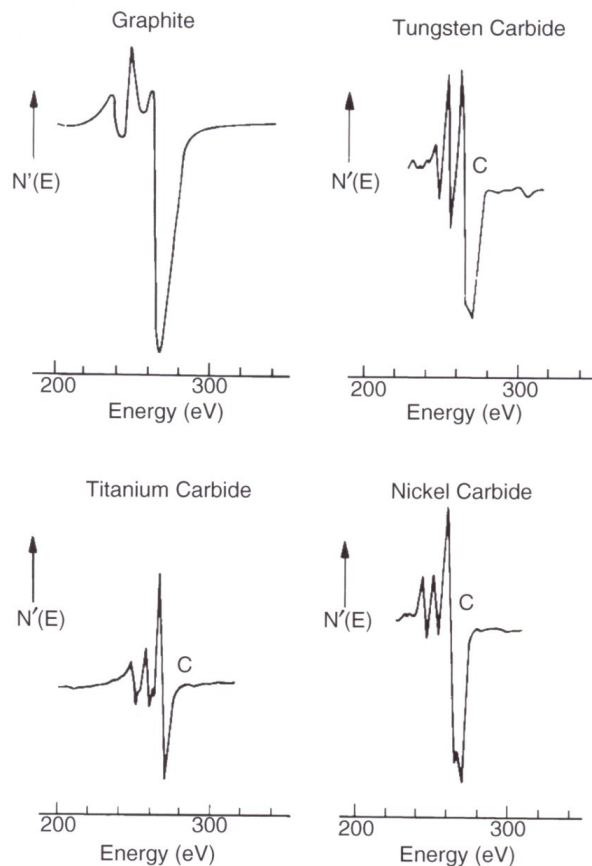
Wikipedia



9-channel
channeltron array
Dr. Sjuts
Optotechnik GmbH

Effects of atomic binding on AES lineshapes

Example: carbon KVV Auger line at ~ 270 eV



Briggs, Grant: Surface Analysis by Auger and X-ray Photoelectron Spectroscopy

AES for quantitative determination of elemental concentrations

- Sensitivity factors
 - Sensitivity factors in analogy to XPS
 - Reference: intensity I_{Ref}^{∞} of Ag MNN transition (sensitivity factor = 1)
 - Sensitivity factors of other Auger transitions:

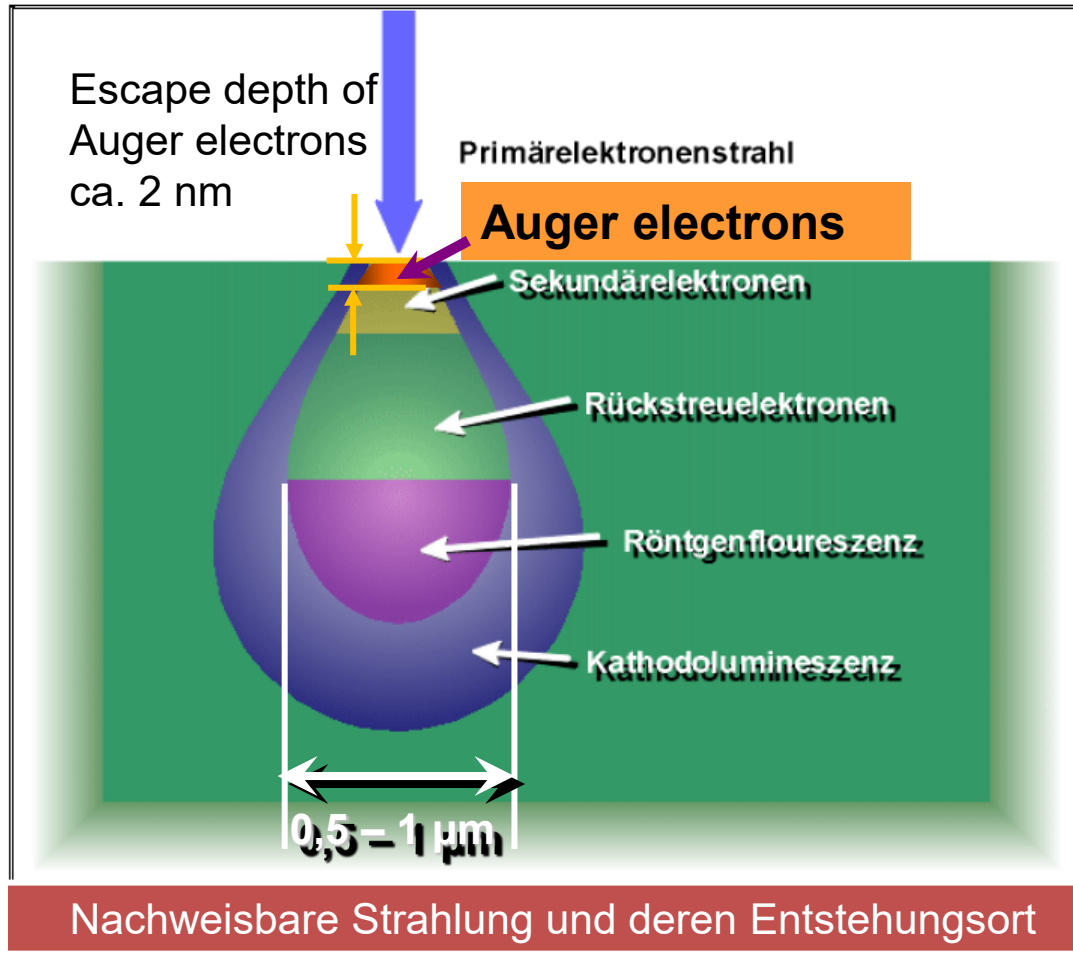
$$S_k = \frac{I_k^{\infty}}{I_{Ref}^{\infty}}$$

- Concentration of element A:

$$c_A = \frac{\frac{I_A}{S_A}}{\sum_{k=A,B,\dots} \frac{I_k}{S_k}}$$

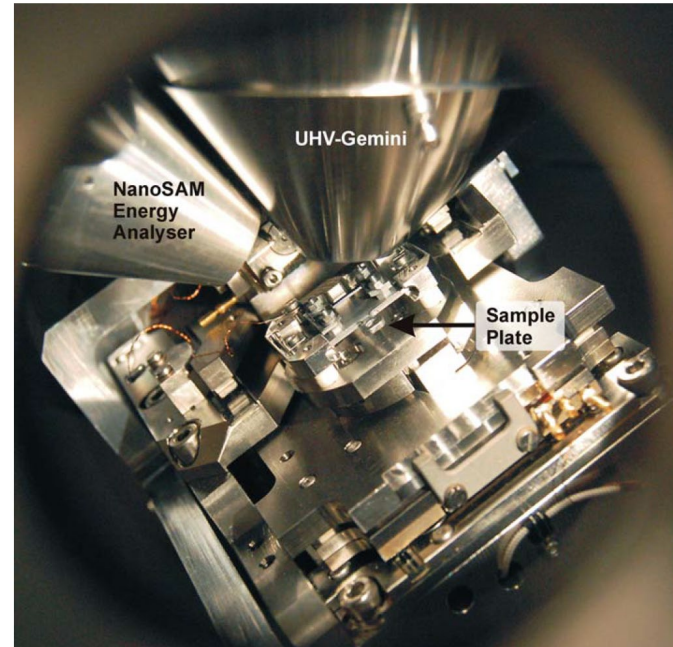
- Formular applicable only for **homogeneous distribution of elements** and for Auger transitions of **comparable mean free paths** (similar to XPS)

Electrons generated by primary electron beam of keV energy



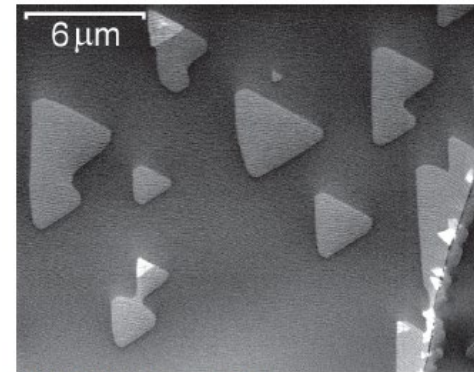
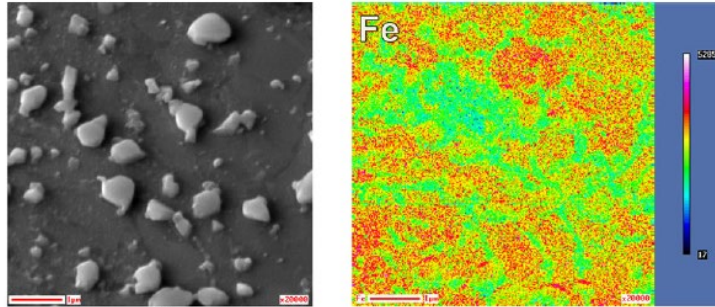
- Spatial resolution by excitation with a well-focussed electron beam (diameter < 1 nm)
- Probed volume has diameter of ca. 1 µm
- Auger electrons escape the sample towards the detector only from a near-surface region of about 2 nm depth
- Volume accessed with SAM $\approx 5 \cdot 10^{-25} \text{ m}^3$ ($\triangleq \varnothing 20 \text{ nm}$ lateral)
- Comparison with X-ray fluorescence (EDX): $\approx 10^{-18} \text{ m}^3$

Our scanning Auger microscope (SAM, „nanoSAM“)



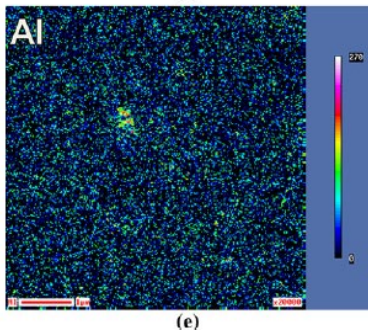
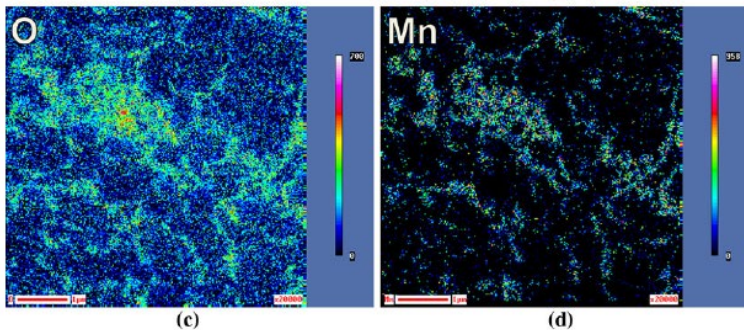
Application examples of SAM

Segregation of **sulfur** bulk contaminations to the surface of a Fe-Ni polycrystal (Dissertation B. Borkenhagen TU Clausthal 2012)



SEM

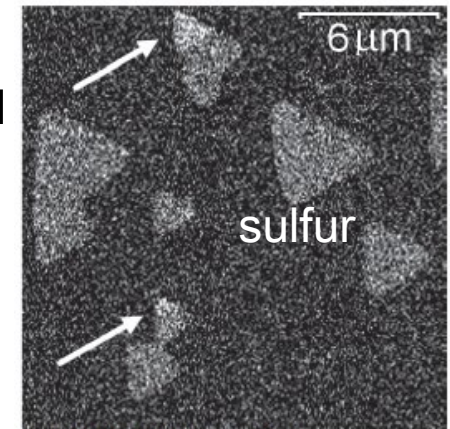
(c) SEM-Bild, $E_P = 5 \text{ keV}$



Chemical surface composition of a steel surface

Bellhouse and McDermid, Metall. Mater. Trans. A 42A (2011), 2753

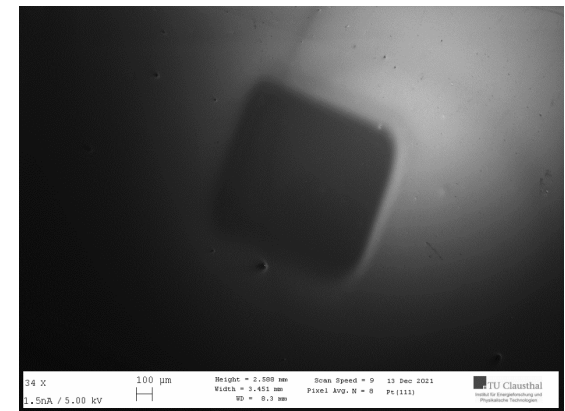
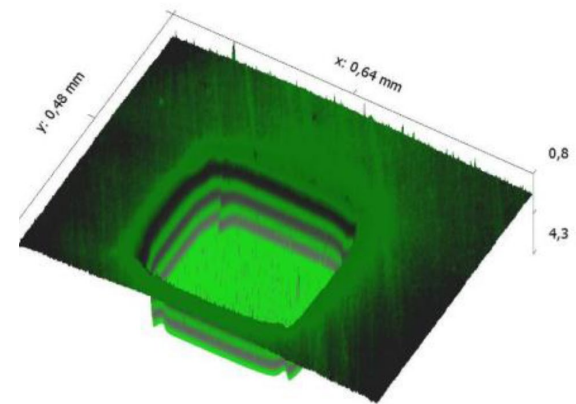
SAM



Summer Sch (e) SAM-Bild, $E_P = 5 \text{ keV}$, $E_{\text{Auger}} = 150 \text{ eV}$ (Schwefel)

Depth profiling of chemical elements with AES

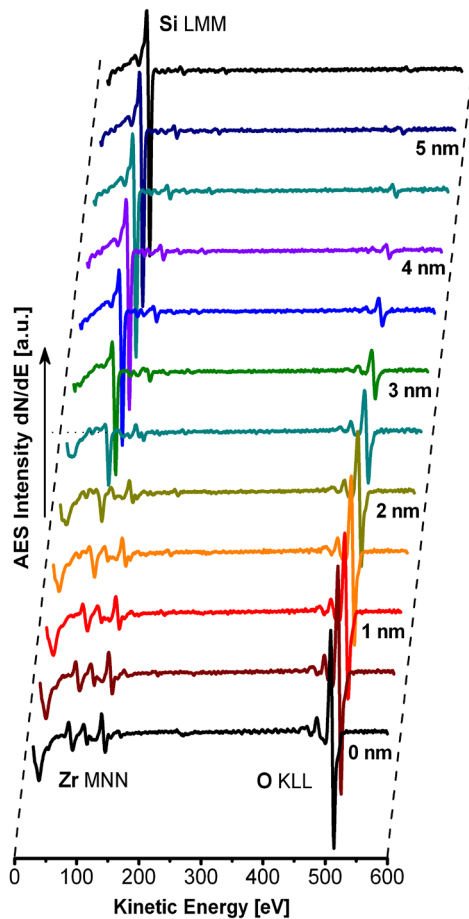
- Layer-by-layer removal of material by ion sputtering = ion etching
- Rasterizing a fine etching ion beam across a sufficiently large sample area causes a crater with a plane ground
- Depth profile: concentrations of relevant elements (determined by AES) as a function of sputter depth
- By suitable calibration measurements, the etching time can be converted to etching depths. For this purpose, the depth of the sputter crater is measured with a profilometer
- Applications of AES depth profiling: determination of **material diffusion** (for example as a result of welding processes), **thickness determination of thin deposited layers**, **surface oxides** or **segregated layers**, characterization of **thin-layer structures in semiconductor heterostructures**



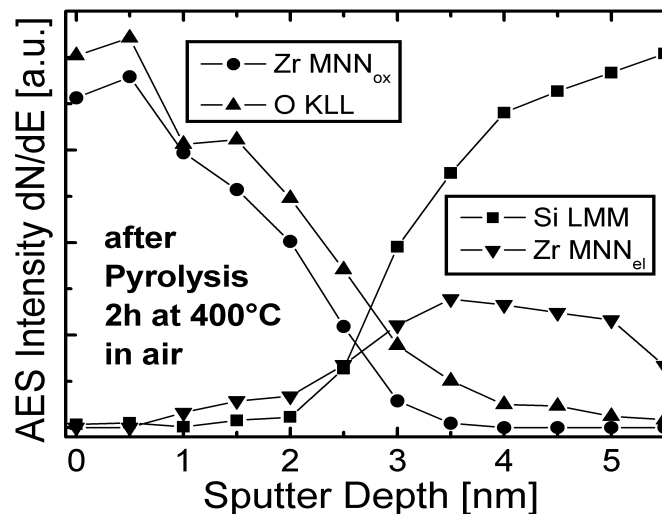
Eggers, Gärtig: Praktikumsversuch

AES depth profiling of a $\text{ZrO}_2/\text{Si}(001)$ heterostructure

- Preparation of a ZrO_2 layer on $\text{Si}(001)$ by a sol-gel process and pyrolysis



Zr (MNN)oxidic: 141 eV
 Zr (MNN)elemental: 148 eV
 Si (LMM): 92 eV

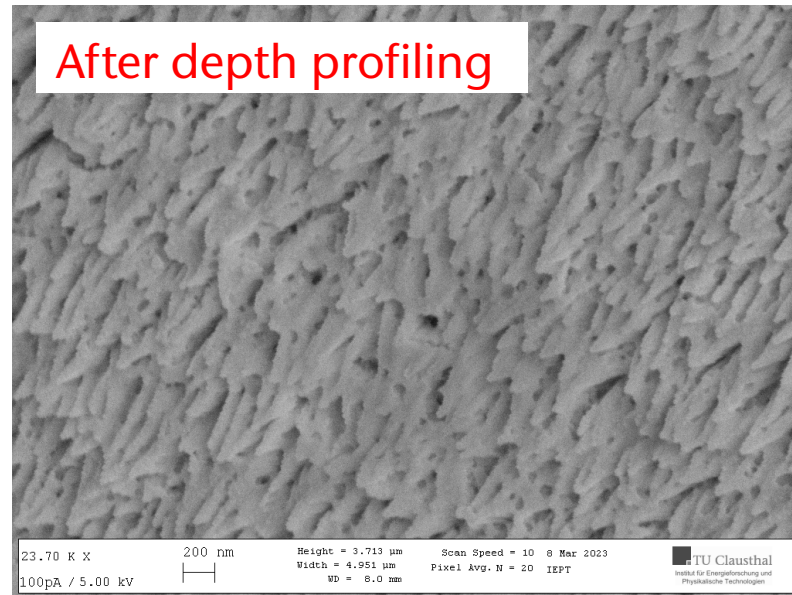
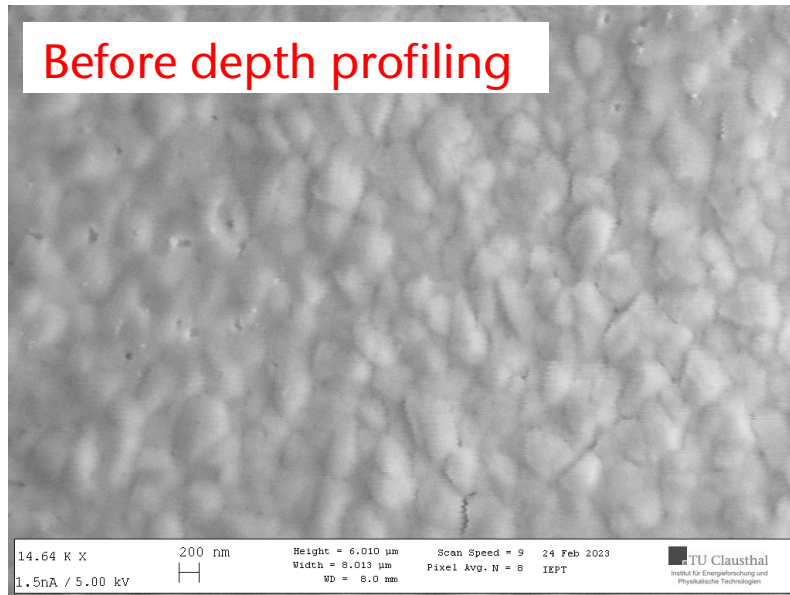


H. Döscher et al., Journal of Applied Physics 107, 094103 (2010)

Artefacts in depth profiling

- Implantation of primary ions
- **Implantation of material** from the surface to deeper regions
- **Ion beam-induced mixing of material** originating from different layers
- **Prefential sputtering**
 - Atoms of a certain element are preferentially removed by ion sputtering
 - Change of concentrations
- **Change of surface topography**, surface roughening by ion etching

Topographical changes by ion etching



Change of the topography of a perovskite semiconductor material by ion etching (SEM images)